Lnk Deficiency Enhances Translesion Synthesis to Alleviate Replication Stress and Promote Hematopoietic Stem Cell Fitness

Brijendra Singh ^{1,2,#}, Md Akram Hossain ^{1,2,#}, Xiao Hua Liang ^{1,2}, Jeremie Fages ^{1,2}, Carlo Salas Salinas ^{1,2}, Roger A. Greenberg³, and Wei Tong ^{1,2,4,*}

- Division of Hematology, Children's Hospital of Philadelphia, Philadelphia, PA 19104
- Division of Pediatrics, Perelman School of Medicine at the University of Pennsylvania, Philadelphia, PA 19104
- Division of Cancer Biology, Perelman School of Medicine at the University of Pennsylvania, Philadelphia, PA 19104
- ⁴ Lead Contact
- [#] These authors contributed equally to this work

Wei Tong, PhD Children's Hospital of Philadelphia, Abramson Bldg. 310D, 3615 Civic Center Blvd., Philadelphia, PA 19104 Tel: 267-426-0930

Email: tongw@chop.edu

Keywords

Hematopoietic stem cells (HSCs), Fanconi Anemia, replication stress, translesion synthesis, DNA replication, DNA damage response, DNA repair, DNA damage tolerance, stem cell fitness.

Running title: LNK regulates replication stress in HSCs

The authors declare no competing financial interest.

^{*} Correspondence author:

Summary

The adaptor protein LNK/SH2B3 negatively regulates hematopoietic stem cell (HSC) homeostasis. *Lnk*-deficient mice show marked expansion of HSCs without premature exhaustion. Lnk deficiency largely restores HSC function in Fanconi Anemia (FA) mouse models and primary FA patient cells, albeit protective mechanisms remain enigmatic. Here, we uncover a novel role for LNK in regulating translesion synthesis (TLS) during HSC replication. Lnk deficiency reduced replication stress-associated DNA damage, particularly in the FA background. Lnk deficiency suppressed single-strand DNA breaks, while enhancing replication fork restart in FA-deficient HSCs. Diminished replication-associated damage in *Lnk*-deficient HSCs occurred commensurate with reduced ATR-p53 checkpoint activation that is linked to HSC attrition. Notably, Lnk deficiency ameliorated HSC attrition in FA mice without exacerbating carcinogenesis during ageing. Moreover, we demonstrated that enhanced HSC fitness from Lnk deficiency was associated with increased TLS activity via REV1 and, to a lesser extent, TLS polymerase eta. TLS polymerases are specialized to execute DNA replication in the presence of lesions or natural replication fork barriers that stall replicative polymerases. Our findings implicate elevated use of these specialized DNA polymerases as critical to the enhanced HSC function imparted by Lnk deficiency, which has important ramifications for stem cell therapy and regenerative medicine in general.

Introduction

Hematopoietic stem cells (HSCs) are endowed with the ability to self-renew and differentiate, thus sustaining a lifelong supply of blood cells. Disruption of HSC homeostasis is associated with a variety of human disorders (1, 2). Faithful maintenance of genome integrity in hematopoietic stem and progenitor cells (HSPCs) is crucial to hematopoiesis and suppression of blood cancers. One of the most common inherited bone marrow failure (BMF) syndromes, Fanconi Anemia (FA), is caused by mutations in one of twenty-three FA complement genes. A network of FA proteins cooperates to repair DNA interstrand crosslink (ICL) damage (3) and relieve replication stress (4), resulting in progressive HSPC decline and increased leukemia/ cancer incidence (5, 6).

The adaptor protein LNK (SH2B3) is a negative regulator of HSC homeostasis (7, 8). $Lnk^{-/-}$ mice exhibit elevated blood counts (9), bone marrow (BM) progenitors (10), and a remarkable over 10-fold increase in HSC numbers with superior self-renewal ability (7, 11, 12). $Lnk^{-/-}$ mice are unique in harboring a markedly expanded HSC pool with multi-lineage reconstitution and serial transplantability without premature exhaustion (13). We previously reported that loss of Lnk partially restores HSC function in both FA mouse models and human HSPCs from FA patients (14, 15). Importantly, LNK does not directly participate in ICL DNA repair; rather, its loss ameliorates replication stress (14). The mechanisms by which Lnk deficiency reduces FA severity and promotes HSC fitness remain to be established.

DNA replication stress, defined as the slowing or stalling of replication forks, is considered an emerging hallmark of cancer and a major contributor to genomic instability (16). It is also prevalent in early mammalian development, resulting in genome instability and aneuploidy, constituting a barrier to development (17). Importantly, replication stress is a potent driver of stem cell functional decline (18). Besides exogenous DNA-damaging agents, endogenous sources of replication stress arise from spontaneous DNA lesions, nucleotide imbalance/depletion, RNA–DNA hybrids, transcription–replication conflicts, or difficult-to-replicate genomic features, including fragile sites, repetitive DNA, and secondary DNA structures (19).

DNA damage tolerance (DDT) mechanisms play a key role in maintaining genome stability against exogenous and endogenous stress. DDT utilizes specialized DNA polymerases to bypass DNA lesions, allowing complete replication without replication fork collapse, thus preventing severe DNA damage (20). One such DDT mechanism is translesion synthesis (TLS), where replicative

DNA polymerase is temporarily replaced by one of the TLS polymerases that can replicate across DNA lesions. The human genome encodes 17 DNA polymerases (Pol) (21). While Pols alpha (α), delta (δ), epsilon (ϵ), and gamma (γ) are responsible for replicating the bulk of nuclear and mitochondrial DNA, the rest specialize in translesion and repair synthesis. TLS is a mechanism whereby specialized DNA polymerases tolerate various DNA lesions to allow for the continuation of DNA replication (22). Despite TLS polymerases having higher intrinsic error rates than replicative polymerases, they increase genome stability and reduce tumorigenesis ostensibly because they allow replication to proceed across blocking lesions that otherwise create replication fork collapse and chromosome breaks, which bear far worse consequences (21). TLS polymerases are best characterized by the Y-family, encompassing Pols Kappa (κ), Eta (η), Iota (ι), and REV1. TLS is mediated by two overlapping but distinct pathways, K¹⁶⁴-monoubiquitination of PCNA (Proliferating Cell Nuclear Antigen, a DNA sliding clamp and DNA polymerase processivity factor) or REV1, to recruit TLS polymerases to replication forks (20). TLS polymerases insert bases opposite the lesion as an "inserter". Extension from the incorporated base is largely carried out by B-family polymerase Pol zeta (ζ) complex via REV1 (19). Rev1^{-/-} and Pcna^{K164R} single mutant mice are grossly normal but show compromised HSPC functions (23, 24). Rev1-/-:PcnaK164R double mutant mice are embryonic lethal from hematopoietic failure, indicating a critical role for TLS in hematopoiesis (25).

While best studied for their ability to bypass physical lesions on the DNA, accumulating evidence suggests a non-canonical role for TLS polymerases in coping with various natural replication fork barriers and alleviating replication stress (21, 26, 27). One notable example is Polη, which replicates efficiently and accurately past ultraviolet (UV) pyrimidine dimers. Mutations in the *POLH* gene that encode Polη are responsible for the variant form of xeroderma pigmentosum (XP-V), a rare autosomal recessive disorder characterized by extreme sensitivity to sunlight and a very high incidence of skin cancer (28). Importantly, recent evidence implicates a role for Polη in maintaining chromosomal stability and preventing common fragile site (CFS) breakage during the unperturbed S phase, irrespective of UV damage, implicating it in the resolution of other stresses (29-31). The non-canonical activities of Polη derive from its enzymatic capacity to accommodate a variety of altered DNA structures, including sequences that form hairpins or G-quadruplexes at CFS or telomeric DNA structures (32). These DNA replication impediments would otherwise block replicative DNA Pols (δ and ε). Thus, Polη mitigates replication stress and promotes genome

stability in S-phase cells by carrying out DNA synthesis at difficult-to-replicate regions of the genome that form natural replication fork barriers (32).

In this study, we performed a comprehensive investigation on how *Lnk* deficiency ameliorates HSC defects associated with FA and how *Lnk* deficiency increases HSC fitness in general. Our work uncovered a novel role for the LNK-regulated TLS polymerases in controlling HSC expansion upon replication stress. Our data suggest that the loss of *Lnk* promotes TLS activities to facilitate DNA replication and reduce replication-associated DNA damage, thus reducing ATR/p53 checkpoint activation and HSC attrition. The mechanisms by which *Lnk* inhibition alleviates endogenous replication stress and promotes HSC fitness have important ramifications for stem cell therapy and regenerative medicine in general.

Results

Lnk deficiency reduces DNA damage in *Fancd2*^{-/-} HSPCs at the steady state and upon replication stress

HSPC decline in FA patients is attributed to elevated DNA damage. To explore the mechanisms by which *Lnk* deficiency ameliorates HSPC defects associated with FA, we set out to examine DNA damage at the steady state and upon replication stress under various conditions.

We first measured the phosphorylation of H2AX (pSer139) or γH2AX, a common DNA damage marker, in both HSPC (LSK) and HSC (SLAM LSK) populations at the steady state using fluorescence-activated cell sorting (FACS). *Fancd2*^{-/-} HSPCs indeed had significantly increased γH2AX as compared to wild-type (WT) controls, while *Lnk*^{-/-} HSPCs showed significantly lower γH2AX levels than those of *Fancd2*^{-/-}. Notably, loss of *Lnk* significantly reduced the γH2AX level in *Fancd2*^{-/-} HSPCs (**Figure 1A**). To precisely assess γH2AX on the DNA, we developed a FACS strategy to quantify chromatin-bound γH2AX in HSCs in different cell cycle stages *in vivo* (**Figure 1B**). We injected EdU (5-ethynyl-2'-deoxyuridine) into mice 2 hours prior to BM harvest. BM cells were subjected to Triton-based pre-extraction to remove soluble γH2AX prior to fixation. The cells were stained with antibodies for HSC surface markers and γH2AX followed by Click chemistry-based EdU staining for the cell cycle. *Fancd2*^{-/-} HSCs showed increased γH2AX+% and chromatin-bound γH2AX levels in the S-phase compared to WT, while *Lnk* deficiency

significantly reduced it (Figure 1B). Proliferation-associated stress is a major cause of DNA damage. To test whether deficiency of *Lnk* reduces replication-associated DNA damage in *ex vivo* culture, we purified LSK cells and cultured them in media containing a cocktail of cytokines, then examined yH2AX+ nuclear foci by immunofluorescence (IF) or FACS. A higher mean fluorescence intensity of γH2AX foci was observed in Fancd2^{-/-} HSPCs, with the majority of the cells having more than four yH2AX foci, indicative of prolonged DNA damage in Fancd2^{-/-} HSPCs. Importantly, $Lnk^{-/-}$ and $Fancd2^{-/-}Lnk^{-/-}$ HSPCs had reduced γ H2AX foci (**Figure 1C**). We also measured the YH2AX levels at different time intervals using FACS. HSPCs exposed to X-ray irradiation were analyzed in parallel as a positive control. Fancd2^{-/-} HSPCs had significantly increased yH2AX levels that peaked at day 5. Importantly, the loss of Lnk significantly reduced the yH2AX levels at all time points (Figure 1D). The majority of HSCs are quiescent at the steady state. However, in response to stress signals such as transplantation into lethally irradiated animals, HSCs exit quiescence and undergo extensive proliferation and differentiation. To gain insights into replication-associated DNA damage in vivo, we measured DNA damage of the donor cells at the short-term and long-term post bone marrow transplantation (BMT) (Figure 1E). At days 6 and 10 of short-term BMT, donor Fancd2-/- cells showed significantly increased yH2AX levels compared to those of WT. Of note, loss of *Lnk* significantly reduced the yH2AX levels in Fancd2-/- HSPCs (Figure 1F). Similar results were obtained during long-term replication stress 4 months post BMT (Figure 1G). Furthermore, we examined DNA damage in response to exogenous replication stressors, hydroxyurea (HU), which depletes dNTPs, and camptothecin (CPT), which inhibits topoisomerase I. Freshly-sorted LK (Lineage-ckit+) cells were treated with a graded dose of HU or CPT for 2h, then the cell lysates were subjected to Western blotting (WB) for yH2AX. Both drugs induced yH2AX levels in a dose-dependent manner. The γ H2AX level was more pronounced in $Fancd2^{-/-}$ cells, while Lnk deficiency reduced it (Figure 1H). Together, these data suggest that Lnk deficiency reduced replication-associated DNA damage in Fancd2^{-/-} HSPCs during normal hematopoiesis and upon replication stress.

Lnk deficiency moderately promotes survival of Fancd2^{-/-} mice upon chronic replication stress, and Lnk deficiency does not synergize with FA to exacerbate malignancies during ageing

Since *Lnk* deficiency reduces DNA damage upon short-term replication stress, we next asked if it would also increase resistance to chronic replication stress *in vivo*. Published work from the Milsom lab showed that prolonged forced proliferation by repeated polyinosinic-polycytidylic acid (pIpC) injection induces pancytopenia in *Fanca*-deficient mice (33). We thus subjected WT, *Fancd2*-/-, *Lnk*-/-, and *Fancd2*-/-*Lnk*-/- mice to an extended pIpC regimen, ie, 2 times per week pIpC injection for 4 weeks followed by 4 weeks rest. We repeated this treatment for 7 cycles and found that *Lnk*-/- mice survived significantly longer than WT mice, while *Fancd2*-/- mice died faster (**Figure 2A**). Importantly, *Fancd2*-/-*Lnk*-/- mice survived slightly longer than *Fancd2*-/- mice, and showed no significant difference from that of WT mice (**Figure 2A**).

It has been shown that cumulative rounds of replicative stress in WT mice can precipitate an HSC phenotype akin to accelerated ageing (33). We directly examined the survival of cohorts of WT, Fancd2-/-, Lnk-/-, and Fancd2-/-Lnk-/- mice during ageing. Complete blood counts revealed significantly elevated platelet numbers in aged $Lnk^{-/-}$ mice, similarly to young mice (9, 10, 14). Fancd2^{-/-} mice exhibited normal blood counts upon ageing, similarly to young mice (14, 34). Notably, aged $Lnk^{-/-}$ mice showed a significant expansion of white blood cells accompanied by a slight decrease in red blood cell count (Figure 2B), consistent with our previous reports (35). We previously showed that aged Lnk^{-/-} mice exhibit a myeloproliferative neoplasm (MPN)-like disease, then progress to and succumb to monocytic tumors and, to a lesser extent, B-cell leukemia. (35, 36). In accordance, $Lnk^{-/-}$ mice died slightly earlier than WT mice (Figure 2C). Fancd2^{-/-} mice exhibited a similar life span to WT mice. Notably, Fancd2^{-/-}Lnk^{-/-} mice reduced myeloid and lymphoid expansion, and ameliorated the anemia of $Lnk^{-/-}$ mice (Figure 2B), although we were not able to do a comprehensive study of the pathology of the moribund mice. Nonetheless, $Fancd2^{-/-}$; $Lnk^{-/-}$ mice showed a similar life span to that of $Lnk^{-/-}$ mice (**Figure 2C**). Taken together, *Lnk* deficiency moderately promotes survival of *Fancd2*^{-/-} mice upon chronic replication stress, and Lnk deficiency does not synergize with FA to exacerbate malignancies during ageing.

Lnk deficiency attenuates ATR but not ATM mediated DNA damage response upon replication stress

DNA damage triggers DNA damage response (DDR), which is coordinated by a network of protein kinase cascades, with ATM and ATR being two major branches. The ATM pathway is primarily activated by double-strand DNA breaks (DSBs) and through checkpoint kinase 2 (Chk2). The ATR

pathway is activated by single-strand DNA breaks (SSBs), and the ATR function is dependent on its binding partner ATRIP, which is recruited to ssDNA upon replication stress and subsequently activates checkpoint kinase 1 (Chk1). Both pathways activate p53 to initiate an array of cellular responses, including cell cycle arrest, apoptosis, checkpoint activation, and DNA repair (37). To examine whether LNK regulates DDR, we evaluated the activation of the ATM and ATR pathways in HSPCs. Since the majority of HSCs are in quiescence or slow in the cell cycle, we administered a single dose of pIpC to mice to induce HSCs into the cell cycle and DNA replication. pIpC increased the percentage of HSCs in the S-phase at 24 hours, as previously shown (33) (Supplementary Figure 1). It activated both ATM and ATR pathways (Figure 3 and Supplementary Figure 2). Fancd2-/- HSCs had increased activation of ATR (as indicated by ATRIP and pChk1) and ATM (as indicated by pATM and pChk2) pathways, compared to that of WT HSCs. Lnk deficiency significantly reduced the activation of the ATR but not the ATM pathway. Importantly, loss of Lnk significantly reduced the activation of ATRIP and pChk1 (Figures 3A-C) but not pATM or pChk2 in the Fancd2-null background (Supplementary Figure 2A, 2B). We next measured DDR upon transplantation-induced proliferative stress. Total BM cells from different genotypes were transplanted into lethally irradiated mice, and four months after BMT, activation of ATRIP, pChk1, pATM, and pChk2 was measured within the donor HSPC population. Fancd2-/- HSPCs had increased ATRIP/pChk1 activation upon transplantationinduced stress. Lnk deficiency significantly decreased ATR activation in Fancd2-/-HSPCs (Figures 3D-F). To complement our flow cytometry results by biochemical method to confirm the effect of LNK in regulating the DDR pathways, we treated freshly-isolated LK cells with HU or CPT, then subjected these cells to WB analysis with various phosphor-specific antibodies to the ATM or ATR pathway effectors. Fancd2-/- progenitors had increased activation of both ATR (as indicated by pChk1) and ATM (as indicated by pKAP1) pathways, compared to WT cells. Lnk deficiency reduced yH2AX and pChk1 but not pKAP1 in Fancd2^{-/-} cells (Figures 3G-I). Taken together, these data indicate that *Lnk* deficiency attenuates the ATR pathway activation upon replication stress induced by endogenous stressors (pIpC and BMT) as well as exogenous stressors (HU and CPT).

Lnk deficiency attenuates ATR/p53 checkpoint activation upon replication stress

Upon DNA damage, DDR pathways activate p53, which in turn triggers multiple downstream effects, including cell cycle arrest and apoptosis. Because *Lnk* deficiency reduces the replication stress-induced DNA damage, we sought to investigate the effect of *Lnk* deficiency on p53

activation. P53 was first measured in HSCs at the steady state using flow cytometry. Fancd2^{-/-}HSCs had significantly increased p53 levels, indicating endogenous stress and elevated DNA damage in unperturbed hematopoiesis. Of note, loss of Lnk decreased p53 level in Fancd2^{-/-}HSCs (Figures 4A, B). We further analyzed the impact of Lnk deficiency in regulating the p53 activation during cellular stress. HSPCs were cultured ex vivo in cytokine-containing media, and p53 levels were measured at different time points. Fancd2^{-/-}HSPCs showed significantly higher p53 levels at all the time points, peaking at day 5. Notably, Lnk deficiency significantly reduced the p53 levels (Figures 4C, D). To further examine the effect of Lnk in p53 activation during replication stress, fresh LK cells were treated with HU and CPT and then subjected to WB for p53. Fancd2^{-/-} cells showed increased p53 induction in a dose-dependent manner, while Lnk deficiency reduced it (Supplementary Figure 3). These data correlate with the γH2AX levels, suggesting Lnk deficiency reduces the spontaneous DNA damage, thus reducing DDR and p53 activation in FA.

P53 plays a significant role in restricting HSC expansion upon injury (38), and DNA damageinduced p53 is a major reason for HSPC decline in FA (39). The p53 response is activated in Aldh2 /-Fancd2-/- and Adh5-/-Fancd2-/- HSCs that have elevated endogenous DNA damage, while p53 deletion rescued this accelerated ageing HSC phenotype (40-42). Knockout of p53 also rescued the HSPC defects in Fanca^{-/-} mice (43). Moreover, p53 silencing improves the HSCs' function in human FA cells (39). Our previous studies showed that *Lnk* deficiency restores the phenotypic and functional HSCs in Fand2-/- mice (14). We thus compared the HSC transplant capacity between *Lnk* and p53 deficiency in FA using competitive BMT assays (Figure 4E). Both *Lnk* loss and p53 loss rescued the BM reconstitution defects of Fancd2-/- cells, as we did not find a significant difference in BM reconstitution ability between Fancd2-/-Lnk-/- and Fancd2-/-p53-^{/-} BM cells (Figure 4E, F). However, all *p53*^{-/-} and *p53*^{-/-}Fancd2^{-/-} mice died within 6 months due to T-lymphoma (data not shown). In contrast, loss of *Lnk* did not affect the survival of *Fancd2*⁻ ^{/-} BM transplanted mice, and the Fancd2^{-/-}Lnk^{-/-} transplanted mice showed a significantly increased survival rate than that of p53^{-/-}Fancd2^{-/-} mice (Figure 4G). Notably, loss of Lnk in Fancd2^{-/-} background maintained the BM reconstitution ability for ~ 8 months (Figure 4H). Taken together, these data indicate that loss of Lnk alleviates replication stress-induced DNA damage and ATR/p53 activation, thus improving HSC activity.

ATR signaling is activated by the recruitment of RPA (Replication protein A) to single-stranded DNA (ssDNA) generated through the uncoupling of MCM helicases that continue to uncoil the DNA strand ahead of the slowed/ stalled DNA polymerases upon replication stress (27). Because loss of *Lnk* attenuates the ATR pathway activation upon replication stress, we hypothesize that *Lnk* deficiency reduces ssDNA breaks that trigger the phosphorylation of ATR and its substrates. Freshly isolated LK cells were treated with increasing concentrations of CPT or HU and then subjected to WB (Figure 5A). As previously reported in cell lines (44), loss of *Fancd2* induced the phosphorylation of pSer33-RPA2 and pSer108-MCM2, markers of replication stress and known to be phosphorylated by ATR, in primary HSPCs. Notably, loss of *Lnk* reduced their phosphorylation in *Fancd2*-/- cells. Persistent replication stress leads to severe DNA damage and ATM activation. Indeed, *Lnk* deficiency also attenuated pSer4/8-RPA2, which is a known ATM substrate (Figure 5A and Supplementary Figure 4A).

We next measured the accumulation of RPA2 on the chromatin of the nascent DNA strand from endogenous stress *in vivo*. We injected EdU into mice 2 hours prior to BM harvesting, and the chromatin-bound RPA2 levels were measured in the HSC and MPP populations by flow cytometry (**Figure 5B and Supplementary Figure 4B**). As expected, MPPs exhibited a higher percentage of RPA2+ cells than HSCs, since MPPs are more proliferative than HSCs. A significantly increased RPA2 level was observed in both HSCs and MPPs of *Fancd2*^{-/-} mice. Notably, loss of *Lnk* significantly reduced the RPA2 accumulation in both HSCs and MPPs (**Figures 5C, D**). During replication stress, RPA2 is recruited to, and binds ssDNA generated by stressed or stalled replication forks, thus it peaks at the S phase. To further dissect how the loss of *Lnk* regulates the RPA2 recruitment at the replication fork, we quantified RPA2 levels in different phases of the cell cycle (**Figure 5E**). In MPPs, chromatin-bound RPA2 reached the highest level in the S-phase, where *Fancd2*^{-/-} showed a significant increase in comparison to that of WT. Interestingly, in HSCs, *Fancd2*^{-/-} cells had elevated RPA2 levels in the G0/G1 phase. Of note, *Lnk* deficiency reduced the RPA2 accumulation in both HSCs and MPPs in different cell cycle stages (**Figure 5F**).

The elevated RPA2 level in the G0/G1 phase of Fancd2^{-/-}HSCs could be due to unrepaired DNA damage in the G2/M phase of the previous cell cycle. We thus directly assessed the proportion of cells with ssDNA generated from endogenous replication stress *in vivo*. 16-hr BrdU labeling coupled with antibody staining under non-denaturing conditions was used to measure the ssDNA

on the nascent DNA strands. 2h of EdU labeling at the end of BrdU allowed us to evaluate the ssDNA generated in different phases of the cell cycle (Supplementary Figure 5A and Figure 6A). Replication stress induced by pIpC or IR induced the proportion of ssDNA, as expected (Supplementary Figure 6A). Fancd2^{-/-} HSCs had a higher proportion of cells with ssDNA compared to WT, and this difference was the most pronounced in the S-phase (Figure 6B, C). Importantly, loss of *Lnk* significantly reduced ssDNA% in Fancd2^{-/-} HSCs (Figures 6A-C). Together, these data suggest that *Lnk* deficiency reduces chromatin-bound RPA and ssDNA breaks at the replication forks, leading to reduced ATR activation during endogenous stress.

Lnk deficiency suppresses ssDNA gaps and promotes replication fork recovery at the stalled forks in *Fancd2*^{-/-} HSPCs.

Unrepaired DNA breaks delay or prevent replication restart once DNA damage reagents are removed; thus, we examined replication restart upon stress. Cultured HSPCs were pulsed with BrdU to label nascent DNA at the replication fork and then subjected to 1hr HU to induce replication fork stalling and halt S-phase progression (**Supplementary figure 5B**). We then washed off HU and labeled cells re-entered the S phase with EdU (**Figure 6D**). BrdU⁺ cells are measured as cells present in the first cell cycle, while BrdU⁺EdU⁺ cells are measured for the efficiency of replication fork restart (**Figure 6E**). There was no significant difference in the BrdU incorporation in different groups of HSPCs, suggesting a comparable proliferation rate among the groups in the short-term culture. However, *Fancd2*-/- HSPCs had reduced EdU% within the BrdU⁺ population, indicating a significant defect in replication restart upon HU treatment. Importantly, *Lnk* loss significantly overcame this defect and restored replication restart in *Fancd2*-/- HSPCs to that of WT levels (**Figure 6E**).

To directly examine fork stalling versus fork recovery upon replication stress, we subjected freshly isolated LSK cells to a fork recovery assay in single-molecule DNA fibers analysis (45, 46). LSKs were pulse-labeled with IdU and then subjected to high-dose HU-mediated replication fork stalling. We then washed off HU and pulsed the cells with CIdU. Single DNA fibers were spread onto microscope slides before immunofluorescence staining with antibodies against CldU and IdU to quantify stalled (IdU or red only) or recovered (IdU-CIdU or red-green) forks. *Fancd2*^{-/-} HSPCs had significantly increased stalled forks (**Figure 6F**). *Lnk* loss significantly overcame this defect and restored replication restart in *Fancd2*^{-/-} HSPCs to that of WT levels (**Figure 6F**).

To directly measure ssDNA gaps in freshly isolated LSK cells, we performed the S1 nuclease assay using single-molecule DNA fibers (Fig. 6G). We examined HSPC replication under mild replication, ie, low-dose HU that slows but does not halt replication. Replication tracts of LSKs were sequentially pulse-labeled with IdU followed by CldU in the presence of lose dose HU. Nuclei were then isolated and split into no S1 and S1-treated groups. Single DNA fibers were spread onto microscope slides before IF staining with antibodies against IdU and CldU. Since S1 nuclease only cleaves ssDNA, the CIdU length is used to quantify intact or cleaved DNA fibers, serving as a measure of ssDNA gaps (46). All four groups of HSPCs show similar fiber lengths without S1 treatment, indicating similar fork speeds. Upon S1 treatment, Fancd2-/- HSPCs exhibited a significant reduction in replication fork length, indicating elevated ssDNA gaps in mild replication stress. Importantly, Lnk deficiency significantly suppressed ssDNA gaps in Fancd2-/-HSPCs (Fig. 6G). Thus, our data suggest that *Lnk* deficiency promotes replication fork recovery at the stalled replication forks in high stress and reduces ssDNA gaps and facilitates replication in Fancd2-/- HSPCs under endogenous or mild stress. Taken together, our data suggest that Lnk deficiency reduces ssDNA breaks and promotes replication fork recovery at the stalled replication forks in *Fancd2*^{-/-} HSPCs.

The superior reconstituting activity of Lnk-- HSCs depends on REV1-mediated TLS

To examine the mechanisms by which Lnk loss ameliorates replication-associated DNA damage, we turned to TLS, one of the DNA damage tolerance (DDT) mechanisms that utilize specialized DNA polymerases to bypass DNA lesions or facilitate replication through replication fork impediments, thus preventing the stalling of DNA replication and the exacerbation of DNA damage (20). TLS is mediated by PCNA monoubiquitination or REV1-dependent pathways (20). While REV1 has a catalytic role in TLS, its major role is to act as a chaperone to recruit other TLS polymerases, such as Pol η /Poli/Pol κ , to the sites of DNA stress and to facilitate switching between the inserter DNA polymerase and the extender DNA polymerase Pol ζ . The REV1-dependent recruitment of Pol η to stalled forks is particularly important for 'on-the-fly' TLS upon replication barriers (32, 47). Therefore, we first examined the sensitivity of Lnk-deficient HSPCs to REV1 inhibition using a small molecule inhibitor, REV1i (JH-RE-06), that disrupts its ability to recruit Pol ζ (48). We plated WT and Lnk- $^{-}$ BM cells in semi-solid methylcellulose cultures containing a graded dose of REV1i. While REV1 inhibition reduced the clonogenic ability of both WT and Lnk- $^{-}$ BMs, Lnk deficiency conferred reduced sensitivity to REV1i (Fig. 7A). We next examined the

HSC repopulation ability upon REV1 inhibition. HSCs (CD150+CD48-LSK or SLAM-LSK cells) from WT and $Lnk^{-/-}$ mice were sorted into 96-well plates and treated with 5uM REV1i or DMSO vehicle control for 3 days. We then transplanted each well into each lethally irradiated recipient mouse (**Fig. 7B**). HSCs appear to be more sensitive to REV1i than progenitors. REV1i significantly reduced the expansion and repopulation ability of both WT and $Lnk^{-/-}$ HSCs (**Fig. 7C**). Notably, REV1i reduced $Lnk^{-/-}$ HSCs to a level similar to that of WT HSCs (**Fig. 7C**). This suggests that the superior reconstituting activity of $Lnk^{-/-}$ HSCs depends on REV1-mediated TLS.

Lnk deficient HSCs have increased chromatin-bound Poln, but their superior reconstituting activity largely does not depend on Poln alone

REV1 recruits multiple specialized TLS DNA polymerases, such as Poln, that play pivotal roles in mitigating a wide range of DNA replication impediments during DNA replication. Examination of our prior genome-wide gene expression data (13) revealed that the mRNA expression level of various DNA polymerases is unchanged in *Lnk*^{-/-} HSCs compared to WT HSCs. We thus examined the protein level of TLS polymerases in Lnk-- HSCs. Due to the antibodies' availability for intracellular flow cytometry, we examined Poln and Polδ1. We found that Lnk-/- HSCs had increased chromatin-bound Polη but not Polδ1 (a replicative DNA polymerase), implicating their enhanced TLS activity through Poln (Fig. 8A-B). To test that, we assessed whether HSCs are sensitive to PolH depletion in vivo using the viral infection/BMT model using two different shRNAs to PolH (Figure 8C-F). Sorted LSKs from WT and Lnk-- mice were infected with lentiviruses expressing miR30-based shRNA against *PolH* or Luc (Luciferase) with mCherry as a marker, followed by transplantation into lethally irradiated recipient mice (Figure 8D). The four experimental groups had similar infection rates at the time of transplantation, as shown by mCherry+ % (Supplementary Figure S6). We quantified mCherry% in the donor population of the peripheral blood of recipient mice to examine HSC activity in vivo. PolH depletion in WT HSCs significantly reduced stem cell repopulating ability; in contrast, Lnk-1- HSCs were more resistant to *PolH* depletion by both shRNAs, exhibiting superior reconstitution ability to WT HSCs (Figure 8E, F). Notably, the stronger PolH depletion via shPolH #1 moderately reduced Lnk^{-/-} HSCs, but only in the short-term transplants (Figure 8F). REV1 recruits other TLS pols, such as Polt and Polk, in addition to Poln, implicating redundant roles of different TLS polymerases in mediating the superior ability of *Lnk*-/- HSCs to mitigate replication stress during regeneration.

Discussion

The adaptor protein LNK is a critical negative regulator of HSC expansion (7, 10-12, 49). We previously showed that loss of *Lnk* restores mouse and human FA HSPCs by alleviating replication stress (14, 15). Understanding LNK regulatory functions in promoting HSC fitness will likely reveal fundamental aspects of stem cell biology. Here, this study uncovers a novel role for LNK in regulating TLS polymerases to control HSC expansion. *Lnk* deficiency mitigates replication-associated DNA damage. This phenotype is more pronounced in the FA background, even in the absence of exogenous DNA damage insults. We show that *Lnk* deficiency suppresses ssDNA breaks and improves replication fork restart, leading to reduced ATR-p53 checkpoint activation that is linked to HSC attrition. Mechanistically, enhanced HSC fitness from *Lnk* deficiency is associated with increased TLS activity via REV1 (**Supplementary Figure S7**). The mechanisms by which *Lnk* inhibition alleviates endogenous replication stress and promotes HSC fitness have important ramifications for other types of BMF syndromes as well as stem cell therapy in general.

This work uncovers that HSPCs utilize TLS DNA polymerases to help alleviate replication stress and promote stem cell fitness. Our data suggest that REV1 and, to a lesser extent, Poln activities contribute to the enhanced HSC fitness observed in Lnk-- HSCs. There are multiple overlapping but distinct TLS pathways and multiple TLS pols; thus, inhibiting one arm of the TLS pathways does not completely block TLS activity. We hypothesize that *Lnk* deficiency has enhanced overall TLS activity, which makes *Lnk*-deficient HSPCs less sensitive to partial TLS inhibition, i.e., Poln knockdown. Moreover, our data does not exclude other TLS-independent mechanisms of mitigating replication stress by Lnk deficiency. Polh^{-/-} mice display no overt defects, except show alterations in antibody hypermutation in B cells (50). XPV patients with *POLH* mutations are not known to develop BMF or leukemia (51, 52). HSPC phenotypes in Polh^{-/-} mice have not been reported. Rev1-/- mice are infertile but grossly normal. Rev1-/- mice showed compromised BMT ability, although it was examined on a mixed background (23). These germline knockout mice may experience compensation during hematopoietic development; thus, HSPC phenotypes would only be manifested upon stress. Our data using shRNA depletion or acute pharmacological inhibitor in adult BM HSCs, subject HSCs to culture and transplantation-associated stress, may account for a more pronounced phenotype. REV1 and Poln function in overlapping but distinct TLS pathways, and REV1 recruits other TLS pols such as Poli and Polκ, in addition to Polη, thus

reducing TLS through one of them may not completely negate the HSC fitness associated with Lnk deficiency. Therefore, it will be important to formally interrogate the potential redundant roles of REV1, Pol η , and other TLS pols in regulating HSC regenerative activity and upon stress in mouse models.

TLS is a type of DDT mechanism that enables specialized TLS polymerases to continue replication in the presence of lesions that otherwise block the replicative polymerases Pol δ or Pol ε. Continued replication, although with an increased error rate, is considered to be better than prolonged fork stalling and fork collapse, which are associated with deleterious DNA damage and structural changes (deletion, insertion, rearrangement), thus genome instability. Recent studies reveal the non-canonical role of TLS pols, in particular Polη, that play important roles in DNA synthesis at undamaged DNA but difficult-to-replicate regions of the genome such as CFS; the generation of immunoglobulin diversity during somatic hypermutation in memory B cells; processing of R-loops during replication-transcription conflict, and maintenance of telomere length through the alternate lengthening of telomeres (ALT) pathway (32). These canonical and non-canonical functions of TLS are crucial mechanisms to protect the genome.

DDT pathways also include template switching (TS), fork reversal, and repriming, besides TLS. K¹⁶⁴-monoubiquitination of PCNA upon DNA lesions is the molecular trigger to switch from the replicative polymerase to the specialized TLS polymerases, to allow the replisome to progress while tolerating DNA damage. Disruption of PCNA K¹⁶⁴-monoubiquitination reduces the recruitment of multiple TLS polymerases. *Pcna^{K164R}* mice show a strong HSC transplant defect, reminiscent of premature aging and stressed hematopoiesis (24). Of note, PCNA is involved in multiple DDT mechanisms; K¹⁶⁴-monoubiquitination is involved in TLS, while K¹⁶⁴-polyubiquitination is involved in template switching (20), both of which contribute to K¹⁶⁴-PCNA's role in HSPCs. Studies of mice deficient in PrimPol, a specialized DNA polymerase for repriming, revealed the requirement of PrimPol for efficient HSC amplification and bone marrow reconstitution (53). DDT warrants continuation of replication through bypassing the impediment to replicate without gaps or repriming downstream of the impediment, then filling ssDNA gaps post-replication (20). TLS polymerases are increasingly being recognized as key players in all DDT mechanisms to mitigate replication stress, critically contributing to genome stability and

cellular fitness (21). Overall, the role of the complex DDT pathways in HSCs emphasizes future investigations.

We previously showed that LNK directly interacts with phosphorylated JAK2 and dampens TPO/MPL/JAK2 signaling in controlling HSC self-renewal (12). Our data in this report suggest that LNK directly or indirectly impacts TLS. However, *Lnk* deficiency may also influence alternative DNA repair pathways. Indeed, TPO was shown to increase DNA repair efficiency in HSCs through an enhanced non-homologous end joining (NHEJ) mechanism upon IR (54, 55). Thus, increased NHEJ and/or homologous recombination (HR) in the absence of *Lnk* may help *FA* or *TLS*-deficient HSC survival. It remains to be formally tested if LNK plays a role in other types of DNA repair in physiologically relevant cells. LNK is a cytoplasmic adaptor protein that is not known to associate with chromatin (12, 36, 56, 57). However, we cannot exclude the possibility that a small fraction of LNK proteins exert functions in the nucleus. The elucidation of how LNK impacts TLS and the recruitment of TLS polymerases to the stressed replication forks is a subject of ongoing investigation.

Our results suggest that enhancing TLS activity could increase the HSC functions by reducing replication-associated DNA damage. One concern of enhancing TLS activity is its error-prone nature on replication through non-damaged DNA templates. Whole genome sequencing of cells lacking components of TLS, such as REV1 or PNCA-Ub, or PrimPol, suggests that TLS and DDT in general protect the genome from deletions and large rearrangements at the expense of spontaneous base substitutions (58). TLS contributes to genetic variance in the human genome. Future studies should conduct in-depth investigations of potential genomic alterations/mutations affected by enhancing TLS activity. Nonetheless, our work sheds light on replication stress amelioration to promote HSC fitness in healthy and disease settings. It also serves as the basis for the future development of small molecules to modulate TLS activities for stem cell therapy. It is important to note that Lnk deficiency reduces DNA damage-mediated ATR/p53 checkpoint activation, preventing HSPC attrition in FA mice upon acute and chronic replication stress. This remarkable ability contrasts with the loss of p53, which was also shown to improve HSC activity in FA. Loss of the tumor suppressor p53 is associated with carcinogenesis and lymphoma in mice. Notably, we show that the combined loss of *Lnk* and *Fancd2* does not reduce survival or increase hematologic malignancies of single *Lnk* knockout mice during ageing. Understanding mechanisms by which Lnk deficiency mitigates replication stress and suppresses DNA damage-induced HSC

attrition will facilitate the development of strategies that have the dual benefit of enhancing HSC fitness and simultaneously reducing genome instability.

Materials and Methods

Sex as a biological variable

Our study examined male and female animals, and similar findings are reported for both sexes.

Mice

Fancd2^{-/-} mice were generously provided by Dr. Alan D'Andrea (Dana Farber Cancer Institute) (34), and *Lnk*^{-/-} mice were obtained by Dr. Tony Pawson (Samuel Lunenfeld Research Institute, Canada) (10), respectively. *Tp53*^{-/-} mice (#002101) were purchased from Jackson Laboratories (59). Both male and female mice (2-6 months) were used in this study. SJL (CD45.1) mice were purchased from the Jackson Laboratory and bred in our facilities. SJL (CD45.1) mice were crossed with C57/B6J (CD45.2) mice to generate CD45.1/CD45.2 F1 mice. All the animal studies were conducted under an approved protocol from the Institutional Animal Care and Use Committee (IACUC) of the Children's Hospital of Philadelphia.

Hematology and flow cytometry of HSPCs and lineage cells

Peripheral blood was collected from the retro-orbital sinus in heparinized tubes. Complete blood count (CBC) was measured using a Hemavet 950 (Drew Scientific). For lineage analysis by FACS, blood cells were lysed using RBC lysis buffer and stained with different fluorochrome-conjugated anti-CD45.1 (A20), -CD45.2 (104), -Gr-1 (RB6-8C5), -Mac1 (M1/70), -CD19 (eBio1D3), -CD3 (17A2). Lineage samples were stained with PI, and acquisition was performed using a BD FACS Canto II flow cytometer. All the data were analyzed using FlowJo.

HSPC staining was conducted as described previously (60). Briefly, cells were quickly lysed with RBC lysis buffer and then stained with biotin-conjugated anti-Gr-1 (RB6–8C5), -Mac1 (M1/70), -B220 (RA3–6B2), -CD19 (eBio1D3), -Ter119 (TER-119), -CD5 (53–7.3), -CD4 (GK1.5), -CD8 (53–6.7), in combination with APC-Cy7-c-Kit (2B8), PerCP-Cy5.5-Sca1 (E13–161.7 or D7), FITC -CD48 (HM48–1), and PE-Cy7-CD150 (TC15–12F12.2) for 30min on ice, followed by secondary staining with streptavidin-PE-TexasRed (Invitrogen SA1017, 1:50). Different HSPC

subpopulations were defined as HSCs (Lin-Sca1+c-Kit+Flk2-CD150+CD48-), and MPPs (CD150-CD48+ LSK) (61). Cells were resuspended in DAPI containing buffer and subjected to flow analysis on a BD FACS Fortessa or Cytek Aurora flow cytometer.

Flow cytometry of intracellular antigens

Briefly, single-cell suspensions of BM cells were obtained by the hind limb together with pelvic bones. Cells were enriched for lineage negative using the Lineage Cell Depletion Kit (Miltenyi Biotec). Bead-labeled cells were separated by autoMACS pro according to the manufacturer's instructions. Lin- cells were first stained for Live/Dead Fixable Aqua (Invitrogen) followed by surface staining for HSPCs. After surface staining, cells were fixed with Cytofix/Cytoperm buffer (BD Biosciences) for 20 min at 4°C, followed by washing with 1x Perm/Wash buffer (BD Biosciences). Cells were further incubated with Permeabilization buffer plus (BD Bioscience) for 10 min at 4°C. After washing with 1x Perm/Wash buffer, cells were further incubated with intracellular antibodies for 2h at room temperature in the dark with anti-pCHK1 (1:200, Invitrogen #MA5-15145), anti-ATRIP (1:200, Invitrogen #PA1-519), PE-anti-pATM (Ser1981) (1:100, Biolegend #651204), PE-anti-pCHK2 (Thr68) (1:100, Biolegend #12-9508-42), AF488-γH2AX (1:100, Biolegend #613406) and AF488-p53 (1:50, Cell Signaling #2015S). For the unconjugated antibodies, cells were further incubated with Rabbit AF647 secondary antibody (1:250, Invitrogen #A-21244) for 30 min at room temperature. After washing, cells were resuspended in 1x Perm/Wash buffer and acquired on a BD Fortessa flow cytometer.

For the detection of chromatin-bound proteins, EdU (1mg) was injected into the mice intraperitoneally for 2h. Mice were sacrificed, and c-kit positive cells were isolated using CD117 microbeads (Miltenyi Biotec) and stained with PerCP-Cy5.5-Sca1 (D7) and APC-Cy7-CD48 (HM48-1) cell surface markers for 30 min at 4°C. For pre-extraction, cells were washed once with PBS and incubated with ice-cold pre-extraction buffer (PBS containing 0.2% Triton X-100) for 1 min on ice before fixation. Fixation was performed using Cytofix/Cytoperm buffer (BD Biosciences) for 20 min at 4°C. Cells were permeabilized using 1x Perm/Wash buffer (BD Biosciences). Click-iT reaction was performed according to the manufacturer's protocols using AF647 azide, Triethylammonium salt (#A10277), to stain EdU. For the intracellular staining, cells were incubated for 2h at room temperature with anti-RPA2 (1:100, Abcam #ab76420), AF488-γH2AX (1:100, Biolegend #613406), AF488-BrdU (MoBU-1) (1:50, Invitrogen #B35110), anti-

DNA polymerase eta (1:200, Abcam #ab236450) and anti-PolD1 (1:200, Abcam #ab186407). For RPA2 staining, cells were further incubated with Rabbit AF488 secondary antibody (1:250, Invitrogen #A-21244) at room temperature for 30 min. The stained cells were washed, resuspended in 1x Perm/Wash buffer containing DAPI (1µg/ml), and acquired on a BD Fortessa flow cytometer.

For ssDNA detection, 5-Bromo-2'-deoxyuridine (BrdU) (2mg) (Invitrogen) was injected into mice intraperitoneally for 16h, followed by EdU (1mg) for the last 2h. HSPC staining and pre-extraction were performed as described above. BrdU and EdU dual staining was performed using the BrdU flow kit (BD Bioscience), except DNase 1 digestion was omitted, followed by EdU staining (Thermo Fisher Scientific #C10419) per the manufacturer's recommendations and analyzed by flow cytometry.

Bone marrow transplantation

For competitive primary bone marrow transplantation, 0.3′10⁶ total BM cells (CD45.2) were mixed with an equal number of competitors (CD45.1/CD45.2) and retro-orbitally injected into lethally irradiated recipient mice (CD45.1). Peripheral blood samples were collected at four-week intervals, and donor reconstitution was analyzed using flow cytometry. After 16 weeks of primary transplantation, recipient mice were sacrificed, and bone marrow cells were enriched for lineage negative using the Lineage Cell Depletion Kit (Miltenyi Biotec). Cells were first stained for Live/Dead Fixable Aqua (Invitrogen), followed by surface staining. Intracellular staining was performed to determine intracellular proteins within the donor HSPC populations. For the short-term hematopoietic stress, 15′10⁶ total BM cells (CD45.2) were transplanted into lethally irradiated recipient mice (CD45.1). Mice were sacrificed on d6 and d10 post BMT and stained for flow cytometry.

Western blot

For western blot, the cell pellets were directly lysed in 1x LDS sample buffer (Invitrogen) with a reducing agent (Invitrogen) and sonicated for homogenization. Samples were boiled at 90°C for 10 min and then followed the standard western blot protocol. Membranes were incubated with primary antibodies overnight at 4°C, followed by HRP-conjugated secondary antibodies against rabbit or mouse for 1 hour at room temperature. Membranes were developed with ECL (#34095, Thermo Scientific), and images were captured by KwikQuant Imager. The antibodies used in this

study were anti-γH2AX (1:1000, Millipore #05-636), anti-Histone H3 (1:1000, Cell Signaling #3638S), anti-PCNA (1:1000, Cell Signaling #13110S), anti-RPA2 (1:1000, Cell Signaling #2208), anti-pSer4/8 RPA2 (1:1000, Bethyl #A300-245A), anti-pSer33 RPA2 (1:1000, Bethyl #A300-246A), anti-pSer108 MCM2 (1:1000, Bethyl #A300-094A), anti-MCM2 (1:1000, Bethyl #A301-191A), anti-pSer824 KAP1 (1:1000, Bethyl #A300-767A), anti-KAP1 (1:1000, Bethyl #A300-274A), anti-Actin (1:2000, Santa Cruz #sc-8432), anti-p53 (1:1000, Cell Signaling #2524S), anti-pSer345 CHK1 (1:1000, Invitrogen #MA5-15145), anti-CHK1 (1:1000, Cell Signaling #2360S) and anti-DNA polymerase eta (1:200, Abcam #ab236450).

Viral transduction of LSK cells and bone marrow transplantation (BMT)

Sorted LSKs from WT and *Lnk*^{-/-} mice were cultured for two days in SFEM media (StemCell Technologies Inc.) supplemented with 10% FBS (SAFC Biosciences) and cytokines (100 ng/mL mSCF, 20 ng/mL mTpo, 20 ng/mL FLT3L, 20 ng/mL IL6). Lentivirus expressing mir30-based shRNA to Luciferase (Luc) or *PolH* with mCherry as a marker was preloaded twice into a RetroNectin (T100B, TaKaRa)-coated 12-well plate (62). The shRNA sequences were sh*Polh#*1, cgcatttggtgtcactagaaac, and sh*Polh#*2, cccagatcttctcctggcacaa. Cultured LSKs were transferred to the lentivirus-preload plates and incubated for one more day. At day 3, 0.3x10⁶ cultured LSKs (CD45.2) were mixed with 0.6x10⁶ Sca1-depleted competitor BM cells (CD45.1/CD45.2) and injected into recipient mice (CD45.1) that were irradiated with a split dose of 10Gy. A small fraction of infected cells was kept for one more day to evaluate the viral infection efficiency (56). Post BMT, peripheral blood samples were collected every four weeks, and the reconstitution of mCherry+ cells within total peripheral blood and mCherry+ percentages within CD45+ donors were analyzed using LSR Fortessa flow cytometry.

HSC sorting and transplantation

HSC purification and BMT were performed as described previously(14). Briefly, lineage-positive cells were first depleted using a lineage cell depletion kit (Cat# 130-090-858, Miltenyi Biotec). Lineage negative (Lin-) cells were then stained with APC-Cy7-c-Kit (2B8), PerCP-Cy5.5-Sca1 (E13–161.7 or D7), FITC-CD48 (HM48–1), PE-Cy7-CD150 (TC15–12F12.2). 150 HSCs (CD150⁺CD48⁻LSK) were sorted into a round-bottom 96-well plate on a FACS Aria Fusion sorter. HSCs were cultured for 3 days in 5μM REV1i or DMSO as a control. Cells from each well were mixed with 0.6x10⁶ Sca1-depleted competitor BM cells (CD45.1/2) and injected retro-orbitally into lethally irradiated recipient mice (CD45.1). Peripheral blood samples were collected every

four weeks, and donor reconstitution was analyzed on a FACS Fortessa or Cytek Aurora flow cytometer.

Colony assays

Mouse BMs were plated in semi-solid methylcellulose culture (StemCell Technologies, Vancouver, Canada) according to the manufacturer's recommendations with M3434 media. The colony numbers were scored 7-12 days later.

pIpC injection

For repeated pIpC injection, 5mg/kg pI:pC (InvivoGen) was administered i.p. The administration regimen is 2 times per week for 4 weeks, followed by 4 weeks of rest, and this 8-week cycle was repeated 7 times. For a single pIpC injection to induce HSC into the cell cycle, 2mg/kg was administered i.p.

Fork restart flow cytometry assay

Sorted LSK were cultured for 3 days in SFEM media supplemented with 10% FBS together with various cytokines, mSCF (100ng/ml), mTPO (20ng/ml), mIL-6 (20ng/ml) and mIL-3 (20ng/ml) (Peprotech, Inc.). After 3 days, cells were pulsed with 10μM BrdU (Invitrogen) for 10 min to label the S-phase cells. Cells were washed once with IMDM containing 10% FCS and incubated with hydroxyurea (HU 0.5mM) (Sigma) for 1h to halt the S-phase progression. Cells were washed twice and further incubated with 5-Ethynyl-2'-deoxyuridine (EdU 10μM) (Click Chemistry Tool) for 1h to assess the ability to restart the replication within S-phase cells (BrdU-positive). Cells were immediately fixed and stained with cell surface antibodies for PerCP-Cy5.5-Sca1 (D7) and APC-Cy7-CD48 (HM48-1). BrdU and EdU dual staining was performed using the BrdU flow kit (BD Bioscience) with anti-BrdU (MoBU-1, Invitrogen) antibody, followed by EdU staining (Thermo Fisher Scientific #C10419) per the manufacturer's recommendations, and analyzed by flow cytometry.

Single-molecule DNA fiber assay

Fork recovery and ssDNA gap assays of single-molecule DNA fibers were performed similarly to published protocols (63, 64). Briefly, freshly isolated LSKs were recovered in cytokine-containing media for one hour before fiber assay. For the fork recovery assay, replicating DNA was first labeled by a 20-minute pulse with 50µM CIdU (Sigma), followed by the addition of 2mM HU

(Sigma) for 1 hour to stall replication. Cells were then washed and pulsed with 250μM ldU (Sigma) for 20 min. For S1 nuclease assay, replicating DNA was first labeled by a 20-minute pulse with 50μM CIdU, followed by a 40-minute pulse with 250μM CldU in the presence of 20 μM HU. Cells were then collected and washed with CSK buffer and subjected to a 30-minute treatment with or without S1 nuclease. For both assays, cells were lysed directly on silane-coated slides and then tipped to 30° to spread single DNA fibers. Slides were subsequently fixed, and DNA denatured and neutralized. Slides were incubated with anti-CldU (rat, Abcam) and IdU (mouse, BD Biosciences) primary antibodies, followed by goat anti-rat AF488 and goat anti-mouse AF568 (Invitrogen) secondary antibodies. DNA fibers were captured using a 100x or 60x objective on a Nikon Eclipse 80*i* fluorescent microscope and quantified using FIJI software.

Immunofluorescence

Ex vivo cultured HSPCs were fixed with 4% paraformaldehyde for 20 min at 4°C and washed with PBS. Fixed cells were permeabilized with 0.2% Triton X-100 for 5 min on ice. Cells were washed and stained with anti-mouse γH2AX antibody (1:200, Millipore #05-636) for 2h at room temperature, followed by three washes with PBS. Cells were stained with anti-mouse Cy3 secondary antibody (# 715-165-150, Jackson Immunology) for 30 min at room temperature. Cells were washed twice, and nuclei were stained with DAPI. Stained cells were spun onto glass microscope slides and visualized using fluorescent microscopes. All the captured images were analyzed using Fiji software.

Statistics

For all cell culture, CFC assay, and BMT assays, two-tailed Student's t-tests or ANOVA with multiple comparisons were performed. Graphs are presented as mean \pm SEM or mean \pm SD. For DNA fiber ratios in the DNA fiber assays, the Kruskal-Wallis one-way analysis of variance test was used for nonparametric data, and comparisons between individual groups were calculated using Dunn's multiple comparison post-test in PRISM (GraphPad Software Inc.). Statistical significance was determined by Student's *t*-test, and a P value less than 0.05 was considered statistically significant.

Study approval

All the animal studies were performed under a protocol approved by the Institutional Animal Care and Use Committee of CHOP (#2024-0781).

Data availability

Please refer to the Supporting Data Values file containing all of the underlying values for the data presented in the manuscript. There are no large datasets or computer codes associated with this work.

Acknowledgements

WT is supported by NIH grants R01DK127738 and R01HL095675, awards from the Basser Center for BRCA Research, and a distinguished chair in pediatric hematology of CHOP. MAH is supported by the Hematopoiesis training grant (T32 DK007780), and subsequently by TL1DK143326 and U2CDK136784. We are grateful to Dr. Vemika Chandra for technical assistance and helpful discussions on this work. This work is the result of NIH funding, in whole or in part, and is subject to the NIH Public Access Policy. Through acceptance of this federal funding, the NIH has been given a right to make the work publicly available in PubMed Central.

Author contributions

W. T. conceived the project and supervised the studies. W.T., B.S., M.A.H., and R.A.G. designed the experiments and wrote the manuscript with input from all authors. B.S. and M.A.H. performed all the animal experiments with the assistance of C.S. and X.H.L., who did animal husbandry. B.S. performed biochemistry, and JF performed colony assays and DNA fiber assays. X.H.L. performed BMT and peripheral blood sampling.

Declaration of interests

The authors declare no competing financial interests.

REFERENCE

- 1. Jordan CT, McKearn JP, and Lemischka IR. Cellular and developmental properties of fetal hematopoietic stem cells. *Cell.* 1990;61(6):953-63.
- 2. Morrison SJ, Uchida N, and Weissman IL. The biology of hematopoietic stem cells. *Annu Rev Cell Dev Biol.* 1995;11:35-71.
- 3. Kennedy RD, and D'Andrea AD. The Fanconi Anemia/BRCA pathway: new faces in the crowd. *Genes Dev.* 2005;19(24):2925-40.
- 4. Schlacher K, Wu H, and Jasin M. A distinct replication fork protection pathway connects Fanconi anemia tumor suppressors to RAD51-BRCA1/2. *Cancer Cell*. 2012;22(1):106-16.
- 5. Parmar K, D'Andrea A, and Niedernhofer LJ. Mouse models of Fanconi anemia. *Mutat Res.* 2009;668(1-2):133-40.
- 6. Kee Y, and D'Andrea AD. Molecular pathogenesis and clinical management of Fanconi anemia. *J Clin Invest*. 2012;122(11):3799-806.
- 7. Ema H, Sudo K, Seita J, Matsubara A, Morita Y, Osawa M, et al. Quantification of self-renewal capacity in single hematopoietic stem cells from normal and Lnk-deficient mice. *Dev Cell.* 2005;8(6):907-14.
- 8. Buza-Vidas N, Antonchuk J, Qian H, Mansson R, Luc S, Zandi S, et al. Cytokines regulate postnatal hematopoietic stem cell expansion: opposing roles of thrombopoietin and LNK. *Genes Dev.* 2006;20(15):2018-23.
- 9. Takaki S, Sauer K, Iritani BM, Chien S, Ebihara Y, Tsuji K, et al. Control of B cell production by the adaptor protein lnk. Definition Of a conserved family of signal-modulating proteins. *Immunity*. 2000;13(5):599-609.
- 10. Velazquez L, Cheng AM, Fleming HE, Furlonger C, Vesely S, Bernstein A, et al. Cytokine signaling and hematopoietic homeostasis are disrupted in Lnk-deficient mice. *J Exp Med*. 2002;195(12):1599-611.
- 11. Seita J, Ema H, Ooehara J, Yamazaki S, Tadokoro Y, Yamasaki A, et al. Lnk negatively regulates self-renewal of hematopoietic stem cells by modifying thrombopoietin-mediated signal transduction. *Proc Natl Acad Sci U S A*. 2007;104(7):2349-54.
- 12. Bersenev A, Wu C, Balcerek J, and Tong W. Lnk controls mouse hematopoietic stem cell self-renewal and quiescence through direct interactions with JAK2. *J Clin Invest*. 2008;118(8):2832-44.
- 13. Bersenev A, Rozenova K, Balcerek J, Jiang J, Wu C, and Tong W. Lnk deficiency partially mitigates hematopoietic stem cell aging. *Aging Cell*. 2012;11(6):949-59.
- 14. Balcerek J, Jiang J, Li Y, Jiang Q, Holdreith N, Singh B, et al. Lnk/Sh2b3 deficiency restores hematopoietic stem cell function and genome integrity in Fancd2 deficient Fanconi anemia. *Nat Commun.* 2018;9(1):3915.
- 15. Holdreith N, Lee G, Chandra V, Salinas CS, Nicholas P, Olson TS, et al. LNK (SH2B3) inhibition expands healthy and Fanconi anemia human hematopoietic stem and progenitor cells. *Blood Adv.* 2022;6(3):731-45.
- 16. Macheret M, and Halazonetis TD. DNA replication stress as a hallmark of cancer. *Annu Rev Pathol.* 2015;10:425-48.
- 17. Wang N, Xu S, and Egli D. Replication stress in mammalian embryo development, differentiation, and reprogramming. *Trends Cell Biol.* 2023;33(10):872-86.

- 18. Flach J, Bakker ST, Mohrin M, Conroy PC, Pietras EM, Reynaud D, et al. Replication stress is a potent driver of functional decline in ageing haematopoietic stem cells. *Nature*. 2014;512(7513):198-202.
- 19. Sale JE, Lehmann AR, and Woodgate R. Y-family DNA polymerases and their role in tolerance of cellular DNA damage. *Nature reviews Molecular cell biology*. 2012;13(3):141-52.
- 20. Pilzecker B, Buoninfante OA, and Jacobs H. DNA damage tolerance in stem cells, ageing, mutagenesis, disease and cancer therapy. *Nucleic Acids Res.* 2019;47(14):7163-81.
- 21. Paniagua I, and Jacobs JJL. Freedom to err: The expanding cellular functions of translesion DNA polymerases. *Mol Cell.* 2023;83(20):3608-21.
- 22. Yang W, and Gao Y. Translesion and Repair DNA Polymerases: Diverse Structure and Mechanism. *Annu Rev Biochem.* 2018;87:239-61.
- 23. Martin-Pardillos A, Tsaalbi-Shtylik A, Chen S, Lazare S, van Os RP, Dethmers-Ausema A, et al. Genomic and functional integrity of the hematopoietic system requires tolerance of oxidative DNA lesions. *Blood.* 2017;130(13):1523-34.
- 24. Pilzecker B, Buoninfante OA, van den Berk P, Lancini C, Song JY, Citterio E, et al. DNA damage tolerance in hematopoietic stem and progenitor cells in mice. *Proc Natl Acad Sci U S A*. 2017;114(33):E6875-E83.
- 25. Buoninfante OA, Pilzecker B, Spanjaard A, de Groot D, Prekovic S, Song JY, et al. Mammalian life depends on two distinct pathways of DNA damage tolerance. *Proc Natl Acad Sci U S A*. 2023;120(4):e2216055120.
- 26. Tonzi P, and Huang TT. Role of Y-family translesion DNA polymerases in replication stress: Implications for new cancer therapeutic targets. *DNA Repair (Amst)*. 2019;78:20-6.
- 27. Zeman MK, and Cimprich KA. Causes and consequences of replication stress. *Nat Cell Biol.* 2014;16(1):2-9.
- 28. Masutani C, Kusumoto R, Yamada A, Dohmae N, Yokoi M, Yuasa M, et al. The XPV (xeroderma pigmentosum variant) gene encodes human DNA polymerase eta. *Nature*. 1999;399(6737):700-4.
- 29. Bergoglio V, Boyer AS, Walsh E, Naim V, Legube G, Lee MY, et al. DNA synthesis by Pol eta promotes fragile site stability by preventing under-replicated DNA in mitosis. *J Cell Biol.* 2013;201(3):395-408.
- 30. Rey L, Sidorova JM, Puget N, Boudsocq F, Biard DS, Monnat RJ, Jr., et al. Human DNA polymerase eta is required for common fragile site stability during unperturbed DNA replication. *Mol Cell Biol.* 2009;29(12):3344-54.
- 31. Twayana S, Bacolla A, Barreto-Galvez A, De-Paula RB, Drosopoulos WC, Kosiyatrakul ST, et al. Translesion polymerase eta both facilitates DNA replication and promotes increased human genetic variation at common fragile sites. *Proc Natl Acad Sci U S A*. 2021;118(48).
- 32. Bedaiwi S, Usmani A, and Carty MP. Canonical and Non-Canonical Roles of Human DNA Polymerase eta. *Genes (Basel)*. 2024;15(10).
- 33. Walter D, Lier A, Geiselhart A, Thalheimer FB, Huntscha S, Sobotta MC, et al. Exit from dormancy provokes DNA-damage-induced attrition in haematopoietic stem cells. *Nature*. 2015;520(7548):549-52.
- 34. Parmar K, Kim J, Sykes SM, Shimamura A, Stuckert P, Zhu K, et al. Hematopoietic stem cell defects in mice with deficiency of Fancd2 or Usp1. *Stem Cells*. 2010;28(7):1186-95.

- 35. Bersenev A, Wu C, Balcerek J, Jing J, Kundu M, Blobel GA, et al. Lnk constrains myeloproliferative diseases in mice. *J Clin Invest*. 2010;120(6):2058-69.
- 36. Cheng Y, Chikwava K, Wu C, Zhang H, Bhagat A, Pei D, et al. LNK/SH2B3 regulates IL-7 receptor signaling in normal and malignant B-progenitors. *J Clin Invest.* 2016;126(4):1267-81.
- 37. Ciccia A, and Elledge SJ. The DNA damage response: making it safe to play with knives. *Mol Cell.* 2010;40(2):179-204.
- 38. Bondar T, and Medzhitov R. p53-mediated hematopoietic stem and progenitor cell competition. *Cell Stem Cell*. 2010;6(4):309-22.
- 39. Ceccaldi R, Parmar K, Mouly E, Delord M, Kim JM, Regairaz M, et al. Bone marrow failure in Fanconi anemia is triggered by an exacerbated p53/p21 DNA damage response that impairs hematopoietic stem and progenitor cells. *Cell Stem Cell*. 2012;11(1):36-49.
- 40. Pontel LB, Rosado IV, Burgos-Barragan G, Garaycoechea JI, Yu R, Arends MJ, et al. Endogenous Formaldehyde Is a Hematopoietic Stem Cell Genotoxin and Metabolic Carcinogen. *Mol Cell*. 2015;60(1):177-88.
- 41. Garaycoechea JI, Crossan GP, Langevin F, Mulderrig L, Louzada S, Yang F, et al. Alcohol and endogenous aldehydes damage chromosomes and mutate stem cells. *Nature*. 2018;553(7687):171-7.
- 42. Wang M, Brandt LTL, Wang X, Russell H, Mitchell E, Kamimae-Lanning AN, et al. Genotoxic aldehyde stress prematurely ages hematopoietic stem cells in a p53-driven manner. *Mol Cell.* 2023;83(14):2417-33 e7.
- 43. Li X, Wilson AF, Du W, and Pang Q. Cell-Cycle-Specific Function of p53 in Fanconi Anemia Hematopoietic Stem and Progenitor Cell Proliferation. *Stem Cell Reports*. 2018;10(2):339-46.
- 44. Lossaint G, Larroque M, Ribeyre C, Bec N, Larroque C, Decaillet C, et al. FANCD2 binds MCM proteins and controls replisome function upon activation of s phase checkpoint signaling. *Mol Cell*. 2013;51(5):678-90.
- 45. Mukherjee C, Tripathi V, Manolika EM, Heijink AM, Ricci G, Merzouk S, et al. RIF1 promotes replication fork protection and efficient restart to maintain genome stability. *Nat Commun.* 2019;10(1):3287.
- 46. Quinet A, Carvajal-Maldonado D, Lemacon D, and Vindigni A. DNA Fiber Analysis: Mind the Gap! *Methods Enzymol.* 2017;591:55-82.
- 47. Mellor C, Nassar J, Svikovic S, and Sale JE. PRIMPOL ensures robust handoff between on-the-fly and post-replicative DNA lesion bypass. *Nucleic Acids Res.* 2024;52(1):243-58.
- 48. Wojtaszek JL, Chatterjee N, Najeeb J, Ramos A, Lee M, Bian K, et al. A Small Molecule Targeting Mutagenic Translesion Synthesis Improves Chemotherapy. *Cell*. 2019;178(1):152-9 e11.
- 49. Takaki S, Morita H, Tezuka Y, and Takatsu K. Enhanced hematopoiesis by hematopoietic progenitor cells lacking intracellular adaptor protein, Lnk. *J Exp Med.* 2002;195(2):151-60.
- 50. Martomo SA, Yang WW, Wersto RP, Ohkumo T, Kondo Y, Yokoi M, et al. Different mutation signatures in DNA polymerase eta- and MSH6-deficient mice suggest separate roles in antibody diversification. *Proc Natl Acad Sci U S A*. 2005;102(24):8656-61.
- 51. Inui H, Oh KS, Nadem C, Ueda T, Khan SG, Metin A, et al. Xeroderma pigmentosum-variant patients from America, Europe, and Asia. *J Invest Dermatol.* 2008;128(8):2055-68.

- 52. Oetjen KA, Levoska MA, Tamura D, Ito S, Douglas D, Khan SG, et al. Predisposition to hematologic malignancies in patients with xeroderma pigmentosum. *Haematologica*. 2020;105(4):e144-e6.
- 53. Jacobs K, Doerdelmann C, Krietsch J, Gonzalez-Acosta D, Mathis N, Kushinsky S, et al. Stress-triggered hematopoietic stem cell proliferation relies on PrimPol-mediated repriming. *Mol Cell*. 2022;82(21):4176-88 e8.
- 54. de Laval B, Pawlikowska P, Petit-Cocault L, Bilhou-Nabera C, Aubin-Houzelstein G, Souyri M, et al. Thrombopoietin-increased DNA-PK-dependent DNA repair limits hematopoietic stem and progenitor cell mutagenesis in response to DNA damage. *Cell Stem Cell*. 2013;12(1):37-48.
- 55. Guenther KL, Cheruku PS, Cash A, Smith RH, Alvarado LJ, Burkett S, et al. Eltrombopag promotes DNA repair in human hematopoietic stem and progenitor cells. *Exp Hematol*. 2019;73:1-6 e.
- 56. Jiang J, Balcerek J, Rozenova K, Cheng Y, Bersenev A, Wu C, et al. 14-3-3 regulates the LNK/JAK2 pathway in mouse hematopoietic stem and progenitor cells. *J Clin Invest*. 2012;122(6):2079-91.
- 57. Gery S, and Koeffler HP. Role of the adaptor protein LNK in normal and malignant hematopoiesis. *Oncogene*. 2013;32(26):3111-8.
- 58. Gyure Z, Poti A, Nemeth E, Szikriszt B, Lozsa R, Krawczyk M, et al. Spontaneous mutagenesis in human cells is controlled by REV1-Polymerase zeta and PRIMPOL. *Cell Rep.* 2023;42(8):112887.
- 59. Jacks T, Remington L, Williams BO, Schmitt EM, Halachmi S, Bronson RT, et al. Tumor spectrum analysis in p53-mutant mice. *Curr Biol.* 1994;4(1):1-7.
- 60. Lv K, Jiang J, Donaghy R, Riling CR, Cheng Y, Chandra V, et al. CBL family E3 ubiquitin ligases control JAK2 ubiquitination and stability in hematopoietic stem cells and myeloid malignancies. *Genes Dev.* 2017;31(10):1007-23.
- 61. Pietras EM, Reynaud D, Kang YA, Carlin D, Calero-Nieto FJ, Leavitt AD, et al. Functionally Distinct Subsets of Lineage-Biased Multipotent Progenitors Control Blood Production in Normal and Regenerative Conditions. *Cell Stem Cell*. 2015;17(1):35-46.
- 62. Modlich U, Schambach A, Li Z, and Schiedlmeier B. Murine hematopoietic stem cell transduction using retroviral vectors. *Methods Mol Biol.* 2009;506:23-31.
- 63. Ray Chaudhuri A, Callen E, Ding X, Gogola E, Duarte AA, Lee JE, et al. Replication fork stability confers chemoresistance in BRCA-deficient cells. *Nature*. 2016;535(7612):382-7.
- 64. Jiang Q, Paramasivam M, Aressy B, Wu J, Bellani M, Tong W, et al. MERIT40 cooperates with BRCA2 to resolve DNA interstrand cross-links. *Genes Dev.* 2015;29(18):1955-68.

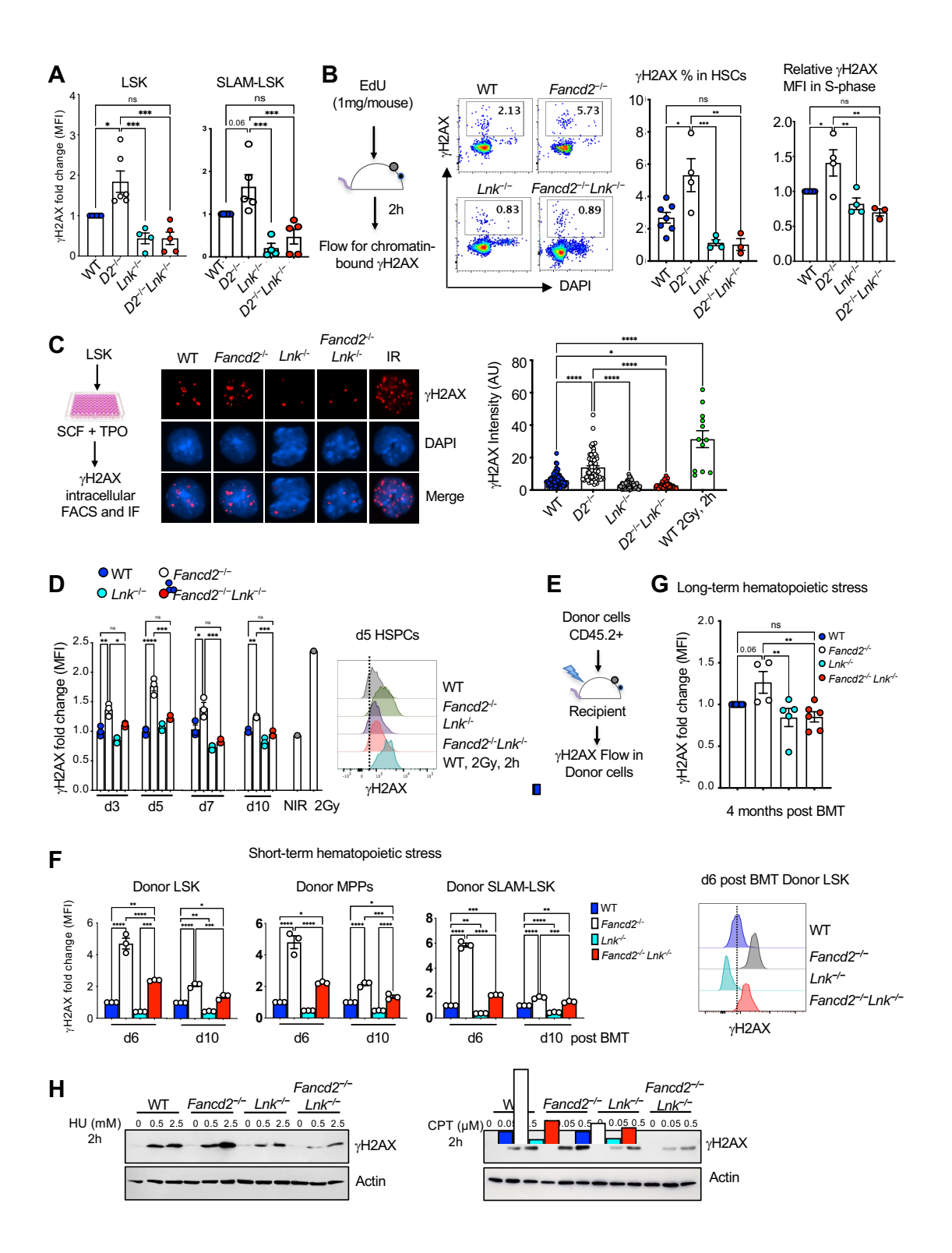


Figure 1. *Lnk* deficiency reduces DNA damage in *Fancd2*^{-/-} HSPCs at the steady state and upon replication stress.

(A-B) Comparison of levels of DNA damage in HSCs and HSPCs at the steady state. (A) Quantification of yH2AX (fold change in MFI as normalized to WT) within LSK and SLAM-LSK populations analyzed by flow cytometry. (B) Experimental design, representative flow cytometry plots, and quantification of chromatin-bound yH2AX within the HSC population. EdU was injected 2 hours before BM harvest, and γ H2AX % and fold change in MFI of γ H2AX within the S-phase of HSCs as determined by EdU+ cells, are shown. (C) Comparison of levels of DNA damage in HSPCs in ex vivo culture. Experimental design for ex vivo LSK culture, representative immunofluorescence images of yH2AX foci, and quantification of fluorescence intensity in d3 HSPCs are shown. IR: irradiated. Magnification: 63X. (**D**) LSKs were cultured, and γH2AX levels were examined by flow cytometry at the indicated days. Quantification of fold change in MFI of γH2AX in ex vivo cultured HSPCs (left) and representative histogram plots for γH2AX in d5 HSPCs (right) are shown. NIR: non-irradiated. WT cells 2h after 2Gy X-ray irradiation were used as a positive control. (E-G) Comparison of levels of DNA damage in HSCs and HSPCs upon replication stress in vivo. (E) Experimental design for YH2AX examination within donor cells of LSK during transplantation-induced replication stress. (F) Quantification of fold changes in MFI of γH2AX within donor LSK, MPPs, and HSCs (SLAM-LSK), d6 and d10 post-BMT (short-term hematopoietic stress), and a representative histogram plot for yH2AX within donor LSK, d6 post-BMT are shown. (G) Fold changes in MFI of \(\gamma H2AX \) within donor LSK, 16 weeks post-BMT (long-term hematopoietic stress) are shown. (H) Immunoblots showing the γH2AX level in freshly sorted LK cells treated with HU or CPT for 2h. In all relevant panels, each symbol represents an individual mouse; bars indicate mean values; error bars indicate SEM. p values were calculated using one-way ANOVA, *, p<0.05; **, p<0.01; ***, p<0.001; ****; p<0.0001.

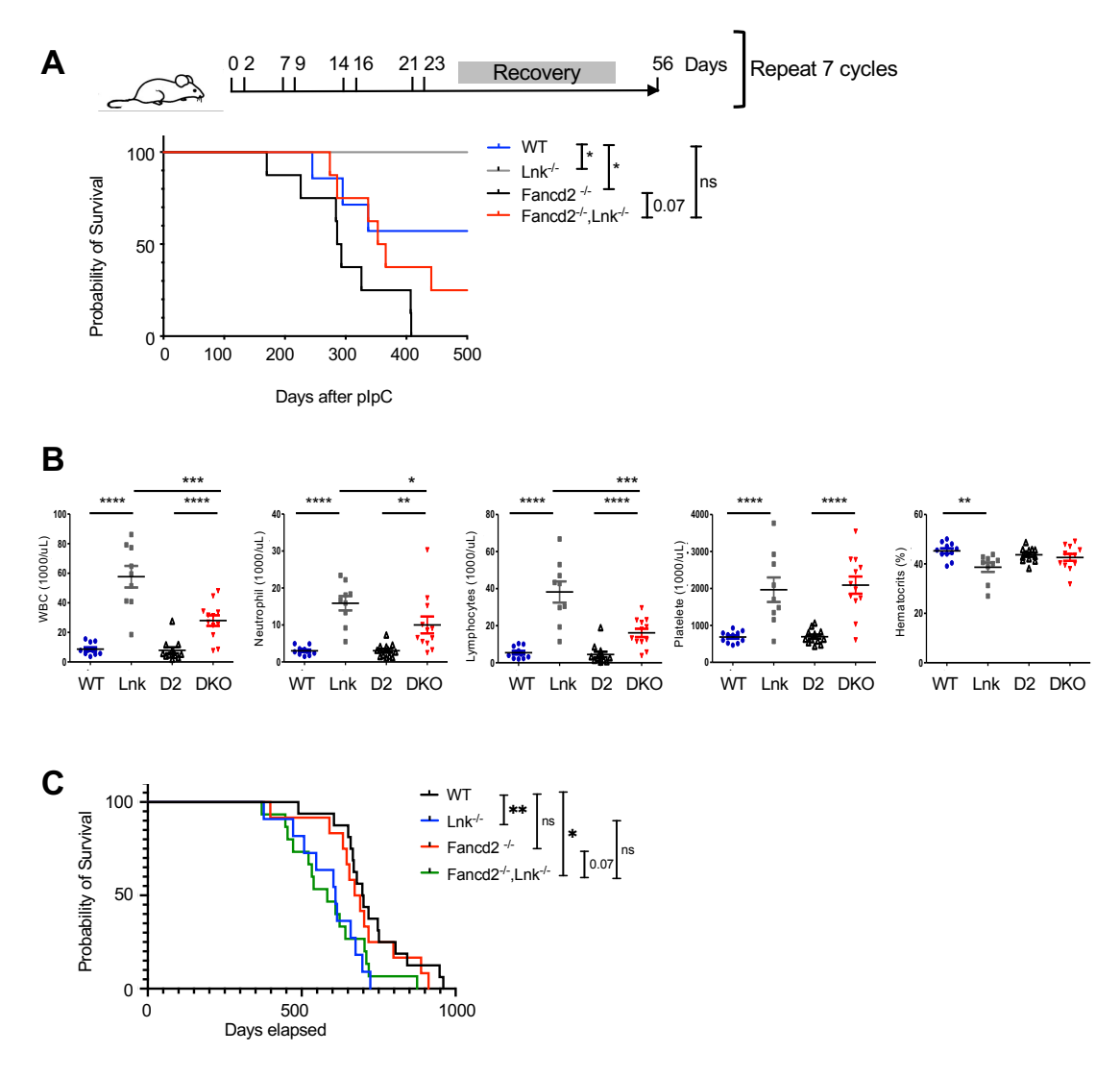


Figure 2. *Lnk* deficiency moderately promotes survival of *Fancd2*— mice upon chronic replication stress, and combined loss of *Lnk* and *Fancd2* does not exacerbate malignancies during ageing.

(A) The top diagram depicts a schematic overview of chronic stress induced by repeated pI:pC injection. Mice were injected i.p. with pI:pC twice per week for 4 weeks, followed by 4 weeks of rest. This 8-week cycle was repeated 7 times. Even-free survival is graphed in Kaplan-Meier curves. n=7-9 mice per group. P values are calculated by log-rank analysis. (B) CBC analysis of peripheral blood from WT, Fancd2-/- (D2), Lnk-/- (Lnk) and FancD2-/-;Lnk-/- (DKO) mice, aged between 12-18 months. WBC: white blood cell. Each symbol represents an individual mouse. Horizontal lines indicate mean frequencies, and error bars indicate SE. p values were calculated using one-way ANOVA, *, p<0.05; **, p<0.01; ***, p<0.001; ****; p<0.0001. (B) A cohort of

mice was observed for ageing analysis. n=11-16 per group. Even-free survival is graphed in Kaplan-Meier curves. P values are calculated by log-rank analysis. *, p<0.05; **, p<0.01; ns, not significant.

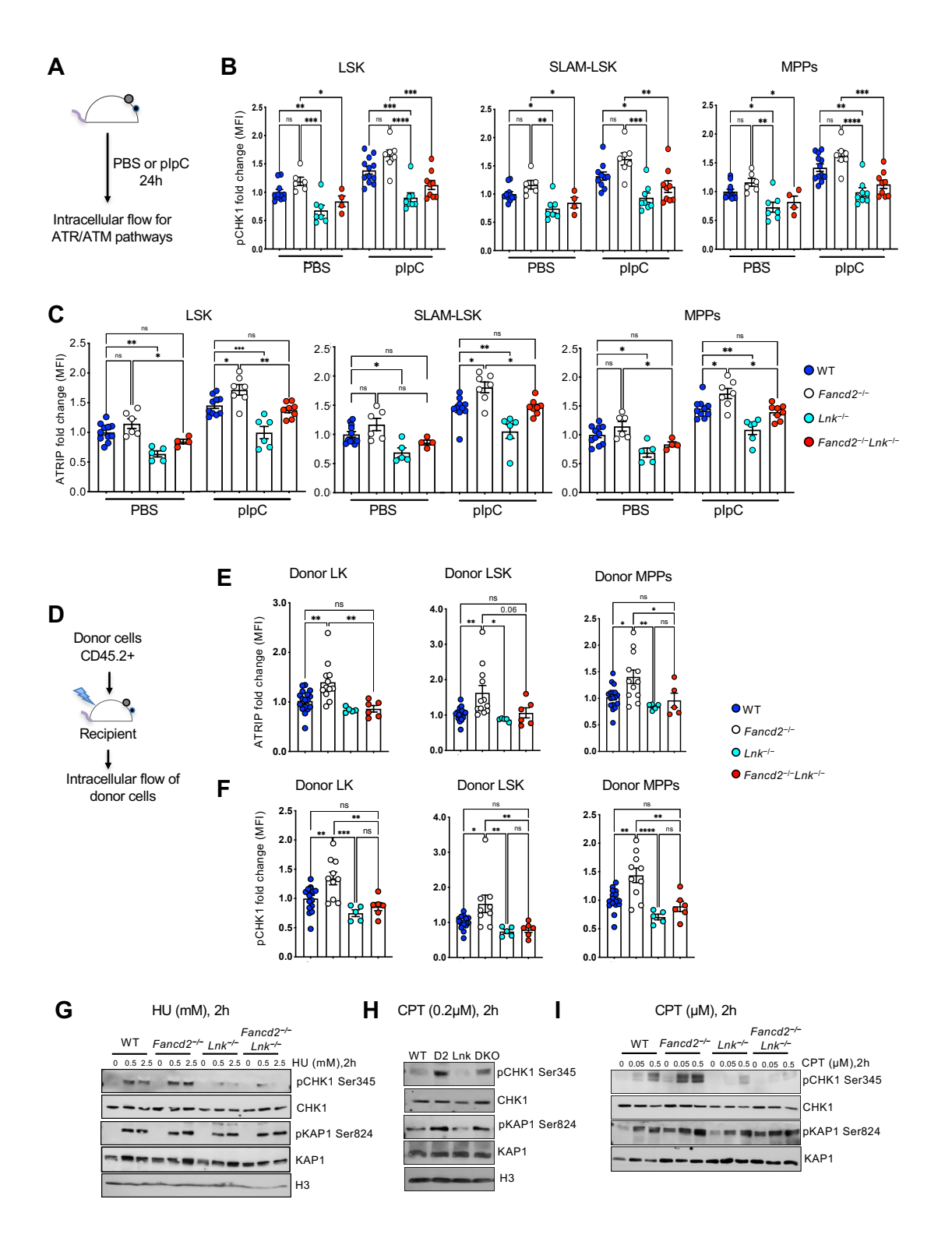


Figure 3. *Lnk* deficiency attenuates the activation of the ATR pathway upon replication stress.

(A) Experimental design for measuring the activation of the ATR pathway upon pIpC-induced HSPC replication. (B-C) Quantification of fold change in MFI of pCHK1 (Ser345) (B) and ATRIP (C) within LSK, SLAM-LSK HSCs, and MPPs populations of PBS and pI:pC administrated mice. (D) Experimental design for measuring the activation of the ATR pathway within the donor HSPC population upon transplantation-induced replication. (E-F) Fold change in MFI of ATRIP (E) and pCHK1 (Ser345) (F) within donor LK, LSK, and MPPs populations after 4 months of BMT. (G-I) Freshly isolated LK cells from WT, Fancd2^{-/-} (D2), Lnk^{-/-} (Lnk), and Fancd2^{-/-}Lnk^{-/-} (DKO) mice were treated with the indicated concentration of HU or CPT for 2h in SFEM containing SCF, TPO, IL-3, IL-6, and the cell lysates were subjected to western blots for different antibodies. The images in I were derived from the same experiment initially shown in Fig. 1H (right panel). In all relevant panels, each symbol represents an individual mouse. Bars indicate mean values, and error bars indicate SEM. p values were calculated using one-way ANOVA, *, p<0.05; **, p<0.01; ****, p<0.001; ****, p<0.001; ****, p<0.001.

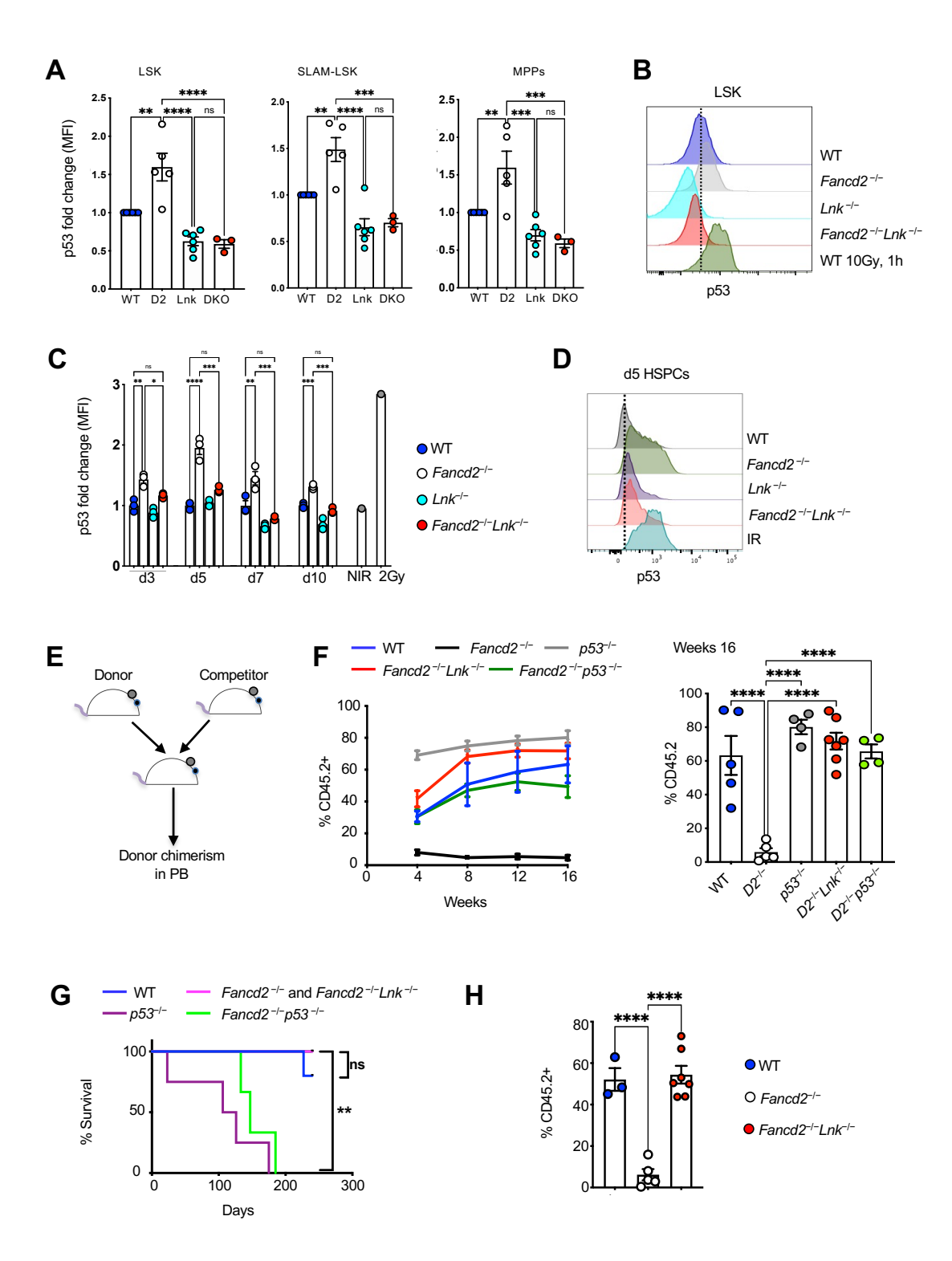


Figure 4. *Lnk* deficiency reduces p53 activation in *Fancd2*^{-/-} HSPCs.

(A) Quantification of p53 levels (fold change in MFI) within LSK, SLAM-LSK HSCs, and MPPs analyzed by flow cytometry. WT, Fancd2^{-/-} (D2), Lnk^{-/-} (Lnk), and Fancd2^{-/-} Lnk^{-/-} (DKO) mice are shown. (B) Representative histogram plots for p53 in the LSK population are shown. WT mice 1h after 10Gy TBI (Total body X-ray irradiation) were used as a positive control. (C) Quantification of p53 (fold change in MFI) in ex vivo cultured LSK of different genotypes at the indicated days. NIR: non-irradiated. IR: irradiated. (D) Representative histogram plots for p53 in LSKs are shown. WT cells 2h after 2Gy X-ray irradiation as a positive control. (E) Experimental design for competitive bone marrow transplantation. (F) The left panel shows the donor chimerism in the peripheral blood over time, and the right panel shows the percentage of donor reconstitution 16 weeks after transplantation. (G) Survival curves of the transplanted mice as in F. (H) Donor chimerism in the peripheral blood of the recipient mice after 32 weeks. In all relevant panels, each symbol represents an individual mouse. Bars indicate mean values, and error bars indicate SEM. p values were calculated using one-way ANOVA, *, p<0.05; **, p<0.01; ***, p<0.001; ****; p<0.0001.

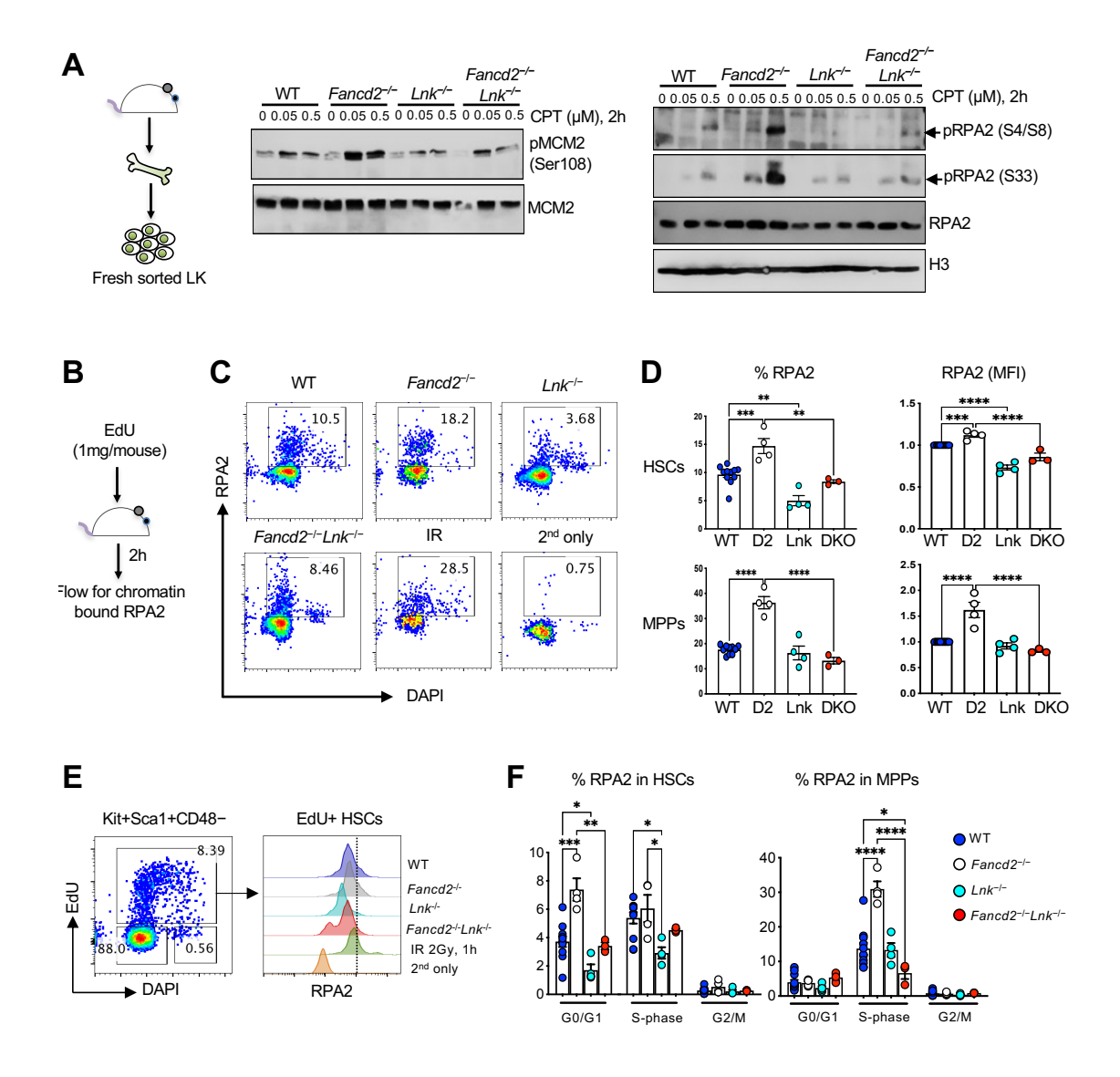


Figure 5. *Lnk* deficiency reduces chromatin-bound RPA in *Fancd2*^{-/-} HSPCs.

(A) Experimental scheme and immunoblots showing the levels of various DDR proteins in freshly sorted LK cells treated with CPT in the presence of cytokines (SCF, TPO, IL-3, IL-6). The images in the middle panel were derived from the same experiment initially shown in Fig. 1H (right panel). (B-D) Comparison of chromatin-bound RPA2 levels in HSPCs upon pIpC-induced replication stress. (B) shows the experimental design, and (C) shows representative flow cytometry plots. IR-induced RPA2 in WT mice is used as a positive control. (D) Quantification of the percentage (left panels) and MFI (right panels) of chromatin-bound RPA2 levels in HSC and MPP populations. WT, Fancd2^{-/-} (D2), Lnk^{-/-} (Lnk), and Fancd2^{-/-} Lnk^{-/-} (DKO) mice are shown. (E) Representative flow cytometry plot showing different cell cycle stages and histogram plot for

chromatin-bound RPA2 within EdU+ HSCs (S-phase) from different mouse groups. **(F)** Percentages of chromatin-bound RPA2⁺ cells in different cell cycle stages of HSCs and MPPs. In all relevant panels, each symbol represents an individual mouse. Bars indicate mean values, and error bars indicate SEM. p values were calculated using one-way ANOVA, *, p<0.05; **, p<0.01; ****, p<0.001; ****; p<0.0001; h, hour.

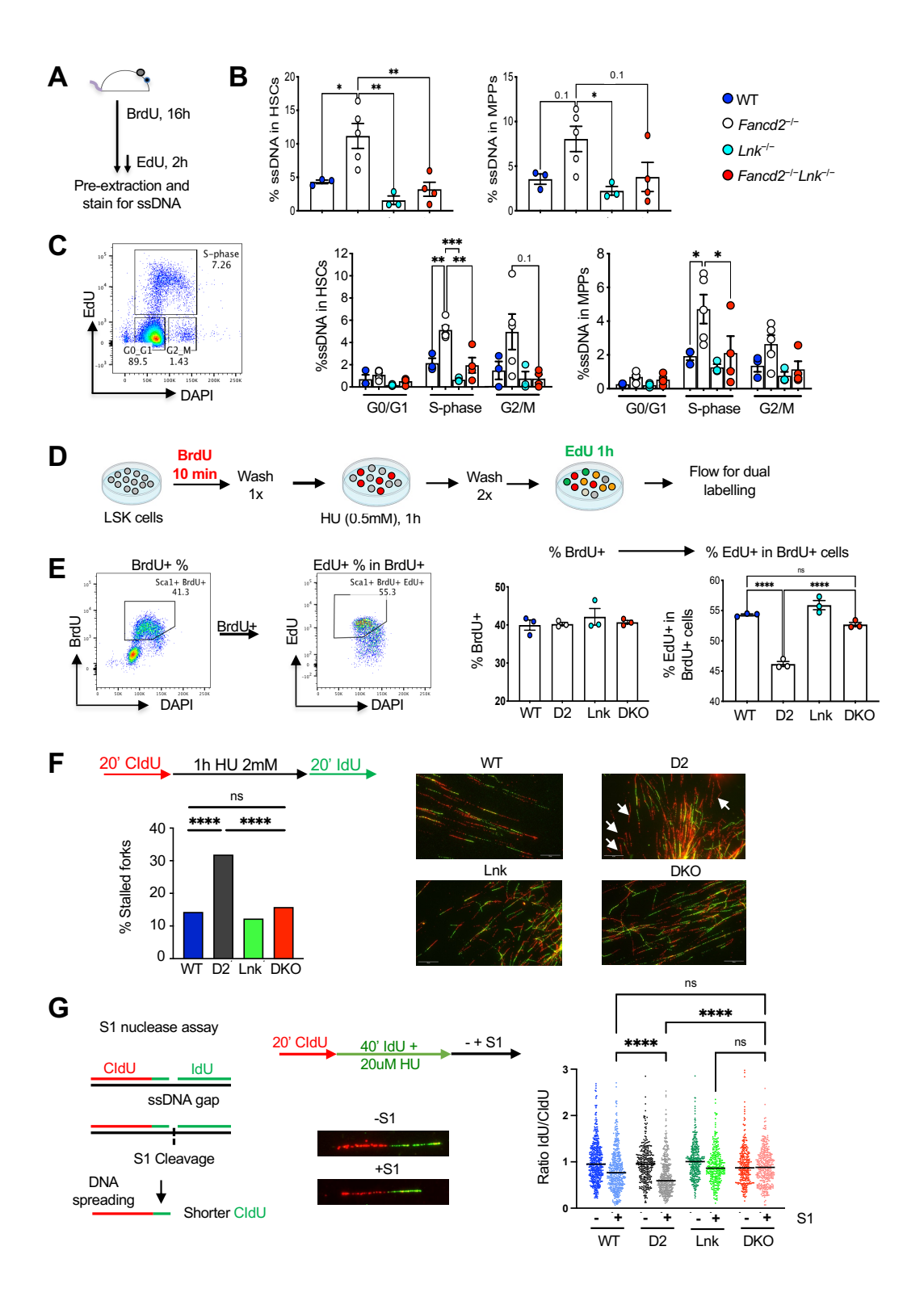


Figure 6. *Lnk* deficiency reduces ssDNA breaks and promotes replication fork recovery at stalled replication forks in *Fancd2*^{-/-} HSPCs.

(A) Experimental design of the experimental procedure to measure ssDNA in vivo. Quantification of total ssDNA within HSCs and MPPs. (C) Representative flow plot showing cell cycle stages and percentage of ssDNA in different cell cycle phases of HSCs and MPPs. (D) Schematic outline of the experimental procedure for the fork restart assay by flow cytometry. (E) Cultured LSK HSPCs from WT, Fancd2^{-/-} (D2), Lnk^{-/-} (Lnk), and Fancd2^{-/-}Lnk^{-/-} (DKO) mice were subjected to the fork restart assay. The left panel shows the representative flow plots of the restarted replication upon HU-induced fork stalling in cultured LSK HSPCs, and the right panel shows the percentages of EdU+ cells from BrdU+ cells of cultured HSPCs. (A-E) In all relevant panels, each symbol represents an individual mouse. Bars indicate mean values, and error bars indicate SEM. p values were calculated using one-way ANOVA, *, p<0.05; **, p<0.01; ***, p<0.001; ****, p<0.0001. ns: non-significant. (F) Freshly isolated primary LSK cells were subjected to fork recovery assay upon HU-mediated replication stalling using single-molecule DNA fibers. The top panel shows the experimental overview of the assay, and the right panel shows representative images of DNA fibers. White arrows indicate stalled replication forks (red only) while the recovered forks show red-green tracks. The frequencies of the stalled replication forks upon high-dose HU-mediated plotted. 175-300 fibers were analyzed per group. Similar results were obtained from two biological repeats. The statistical significance by Fisher's Exact test is shown. (G) Experimental scheme and representative DNA fibers from the D2 group are shown for the S1 nuclease assay to examine ssDNA fibers. Fresh LSK cells from WT, Fancd2^{-/-} (D2), Lnk^{-/-} (Lnk), and D2^{-/-}Lnk^{-/-} (DKO) mice were pulsed with CIdU for 20min followed by IdU in the presence of low-dose HU for 40min. The right panel shows the ratios of IdU/CIdU DNA fibers, with the horizontal lines indicating the geometric mean. 200-500 fibers were analyzed per group. P-values were calculated using Kruskal-Wallis test, *, p < 0.05, **, p < 0.01; ***, p < 0.001; ****, p < 0.0001; ns: not significant. Similar results were obtained from two biological repeats.

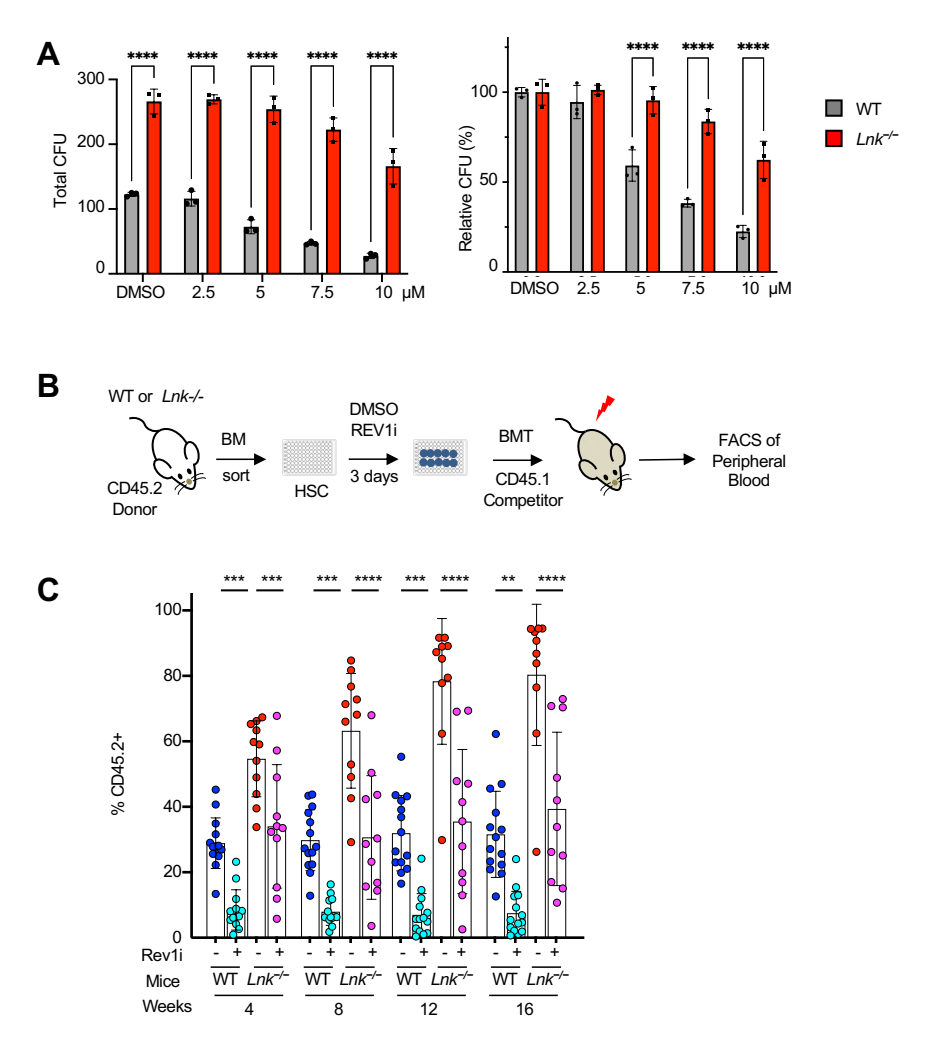


Figure 7. *Lnk*-deficient HSCs are sensitive to REV1 inhibition, and their superior reconstituting activity depends on REV1-mediated TLS.

(A) BM cells from WT and $Lnk^{-/-}$ mice were plated in semi-solid methylcellulose culture containing a graded dose of REV1i in triplicate, at 30K and 15K cells/plate, respectively. Total (left) and relative (right) colony-forming capacities are shown. Mean values and SD are shown. p values were calculated using two-way ANOVA, *, p < 0.05, **, p < 0.01, ***, p < 0.001. (B) Schematic illustration of the lentiviral transduction/BMT experimental scheme. (C) SLAM-LSK HSCs from WT and $Lnk^{-/-}$ mice were sorted into 96-well plates. Cells were cultured in DMSO or 5uM REV1i for 3 days, then cells from each well were transplanted into each lethally irradiated recipient mouse. Donor percentages from each group in the PB are shown. Each symbol represents an individual mouse. Horizontal lines indicate mean frequencies, and error bars indicate SD. p values were calculated using one-way ANOVA, *, p < 0.05, **, p < 0.01, ***, p < 0.001.

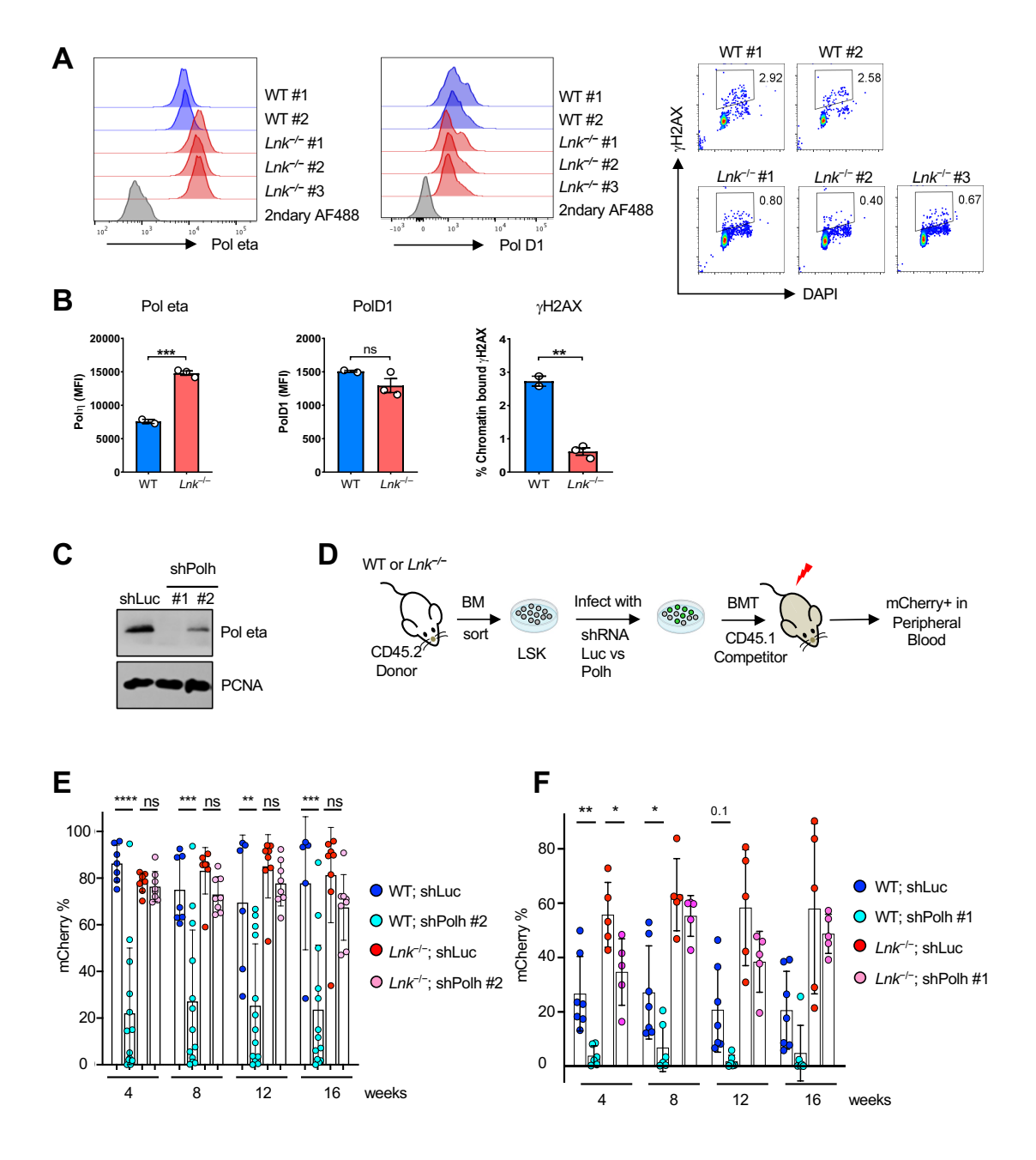


Figure 8. *Lnk*-deficient HSCs have increased chromatin-bound Poln, and their superior reconstituting activity in part depends on Poln.

(A) Representative flow cytometric histogram plots for chromatin-bound Pol eta (left) and Pol delta1 (D1, right) in the HSCs of WT and $Lnk^{-/-}$ mice are shown. (B) Quantification of MFIs of the Pol η , Pol δ 1, and γ H2AX in HSCs as examined in (A). (C) Examination of the efficiency of Pol η depletion using two different shRNAs by WB. (D-F) LSK cells from WT and $Lnk^{-/-}$ mice were infected with lentiviruses expressing shRNA-mediated knockdown of PolH or Luciferase (Luc) as a control and subsequently transplanted into lethally irradiated recipient mice. (D)

Schematic illustration of the lentiviral transduction/ BMT experimental scheme. (E-F) Quantifications of mCherry+ percentages within CD45.2+ donors in the peripheral blood from each group after transplantation using shRNA-PolH#2 (E) or shRNA-PolH#1 (F) are shown. Each symbol represents an individual mouse. Bars indicate mean frequencies, and error bars indicate SD. p values were calculated using one-way ANOVA, *, p < 0.05; ***, p < 0.01; ***, p < 0.001; ns: not significant.